Long-term stable acoustic absorbing boundary conditions for regular-shaped surfaces

Hélène Barucq, Julien Diaz, Véronique Duprat

▶ **To cite this version:**

Hélène Barucq, Julien Diaz, Véronique Duprat. Long-term stable acoustic absorbing boundary conditions for regular-shaped surfaces. [Research Report] RR-8203, INRIA. 2013, pp.34. hal-00776058

HAL Id: hal-00776058
https://inria.hal.science/hal-00776058

Submitted on 18 Jan 2013

HAL is a multi-disciplinary open access archive for the deposit and dissemination of scientific research documents, whether they are published or not. The documents may come from teaching and research institutions in France or abroad, or from public or private research centers.

L'archive ouverte pluridisciplinaire **HAL**, est destinée au dépôt et à la diffusion de documents scientifiques de niveau recherche, publiés ou non, émanant des établissements d'enseignement et de recherche français ou étrangers, des laboratoires publics ou privés.

Long-term stable acoustic absorbing boundary conditions for regular-shaped surfaces.

Hélène Barucq, Julien Diaz, Véronique Duprat

RESEARCH REPORT
N° 8203
January 2013
Project-Team Magique-3D

ISSN 0249-6399 ISRN INRIA/RR--8203--FR+ENG

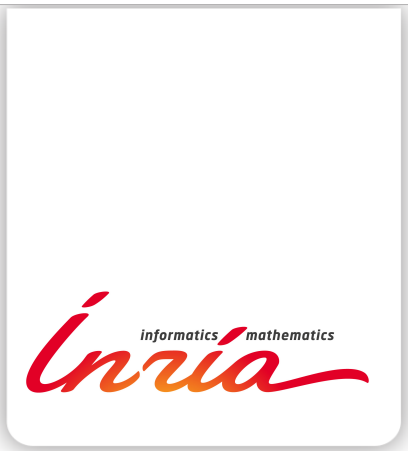

Long-term stable acoustic absorbing boundary conditions for regular-shaped surfaces.

Hélène Barucq*†, Julien Diaz*†, Véronique Duprat†*

Project-Team Magique-3D

Research Report n° 8203 — January 2013 — 33 pages

Abstract: When dealing with regular shaped boundaries, the most widely used Absorbing Boundary Condition is a first-order condition including the curvature of the artificial surface. It is easy to include in variational numerical methods and it performs well. In this paper, we prove that this condition is equivalent to a second-order condition. Actually, we establish that it belongs to a one-parameter family of ABC that lead to well-posed and long-term stable problems. We then propose a 2D performance analysis of the different ABCS, including BGT-like conditions also and we conclude that the first-order condition is the one which performs better.

Key-words: Absorbing boundary conditions; Acoustic wave equation; Well-posedness

* Team-project INRIA Magique-3D INRIA Bordeaux-Sud Ouest, France.
† Laboratory of Applied Mathematics, University of Pau, France.

RESEARCH CENTRE
BORDEAUX – SUD-OUEST

200, Avenue de la Vieille Tour
33405 Talence Cedex

Conditions aux limites absorbantes stables en temps long pour des surfaces régulières

Résumé : La condition aux limites absorbantes (CLA) la plus utilisée pour des frontières courbes régulières est la condition du premier ordre incluant la courbure de la surface artificielle. Elle peut-être facilement prise en compte dans une formulation variationnelle et elle modélise les milieux infinis relativement précisément. Dans cet article, nous montrons qu'elle est équivalente à une condition du second ordre. Nous prouvons en fait qu'elle appartient à une famille de CLA à un paramètre qui mène à des problèmes bien posés et stables. Nous proposons ensuite une analyse de performance des différentes CLA, en incluant également des conditions de type BGT et nous concluons que la condition du premier ordre est la plus performante

Mots-clés : Conditions aux limites absorbantes; Équation des ondes acoustiques; Caractère bien-posé

1 Introduction

The numerical simulation of acoustic waves is often carried out after truncating the propagation domain. The size of the computational domain is then reduced and the spatial approximation can be done with finite element spaces. The corresponding boundary value problem is defined by the coupling of the initial system of equations with a boundary condition set on the external boundary limiting the computational domain. The boundary condition ends the problem and represents the behavior of any wave impinging the external boundary. A "good" condition should be the one for which the numerical waves are not reflected by the external boundary. The computed field would thus be exactly the restriction of the exact wave that propagates inside the larger domain for which the external boundary has been pushed away. The construction of "good" conditions, that are generally called Absorbing Boundary Conditions (ABCs), has been considered in many works. Regarding time-dependent problems, Engquist and Majda [14] have shown that the micro-diagonalization of the wave equation, and more generally of hyperbolic systems, let construct ABCs on arbitrarily-shaped surfaces. The reference work [14] has been followed by a series of papers in which the issue was to derive high-order ABCs to improve the accuracy of the numerical waves by diminishing the amplitude of the reflected waves. For instance, Higdon [18] has derived high-order ABCs which are obtained as the combination of low-order ABCs. Grote and Keller [16] have proposed non reflecting ABCs which are obtained from the approximation of the Dirichlet-to-Neumann (DtN) operator of the sphere. There are many other very interesting papers on the subject and we refer to the review article [27] for a more exhaustive list of references than herein.
Most of the papers addressed the question of constructing ABCs for flat boundaries. It is quite surprising because there exist plenty of applications where the boundary should be curved. For instance, as far as sonar is concerned, it seems more convenient to embed a submarine in an ellipsoid than in a cube. The size of the computational region is then reduced and the computational costs are thus optimized. In the case of harmonic problems, Antoine et al. [4] have proposed a second-order ABC that outperforms the BGT [13] one and obviously any first-order condition. In the case of time-dependent problems, to the best of our knowledge, the same issue has not be addressed and it is not clear that a second-order ABC can perform better than a first-order one. The most widely used first-order condition that is employed for the acoustic wave equation reads as:

$$\partial_n u + \partial_t u + \frac{\kappa}{2} u = 0 \text{ on } \Sigma \times [0, T]. \tag{1}$$

It involves the curvature κ of the boundary Σ. It thus takes the geometry of Σ into account and it is well-known that it performs better than the simplest condition:

$$\partial_n u + \partial_t u = 0 \text{ on } \Sigma \times [0, T]. \tag{2}$$

while both are easy to implement in a variational formulation. Now it is not obvious that condition (1) is outperformed by higher-order conditions in the case of the acoustic wave equation. In [26], it has even been shown that ABCs of order greater than 3 can lead to ill-posed mixed problems. Thus the question of which ABC performs better for the acoustic wave equation remains posed.

Another point to consider is the computational burden that are required by the model. Conditions of high-order are quite easy to implement if we introduce additional unknowns [15]. These latter are only defined on the external boundary. Thus, they do not induce significant computational costs if the number of auxiliary unknowns is low. However, the introduction of a high number of auxiliary unknowns can become problematic by impeding the implementation of parallel computations because it cause hamper the load balancing. Finally, it was recently

shown that we can significantly improve the performance of the ABCs themselves by combining the ABCs with a condition capable of reproducing the evanescent and/or creeping waves [25, 10]. Following these works, it would not be wise to use high-order ABCs. That is why we investigate in this paper the performance of condition 1 compared to higher conditions. More precisely, our goal is to decide if condition 1 is really outperformed by a second order ABC. Regarding the second order ABC, we have decided to use a BGT-like condition. Our choice is guided by the fact that this condition written for monochromatic waves is more efficient compared to other second order conditions [4].

The paper is organized as follows. In section 2, we show how to derive a family of ABCs for the wave equation by applying a micro-diagonalization process that was formerly introduced by M.E. Taylor in [24]. We then get ABCs depending on a parameter γ and at Section 3, we establish that the corresponding mixed problem is well-posed. Moreover, we prove that if $\gamma = \kappa/4$, the condition is equivalent to condition (1), which indicates that condition (1) is more than of order 1. In Section 4, we show that if $\gamma >= \kappa/4$, the corresponding numerical solution behaves like the exact solution, that is the solution converges to zero when the time t goes to infinity. Finally, we address the question of evaluating the numerical performances of each condition. We conduct a performance analysis by comparing the BGT-like condition with the family of ABCs knowing that for $\gamma = \gamma/4$, it corresponds to condition (1). The numerical experiments are carried out with a Discontinuous Galerkin code using a penalized formulation of the wave equation. Our conclusion (1) provides equivalent or better results when compared with all the other conditions, including the BGT-like one.

2 A new family of second-order ABCs for the acoustic wave equation

In this section, we construct a new absorbing boundary condition using the micro-diagonalization method developed by M.E. Taylor [24]. This condition is written for regular domains and takes propagating waves into account. In the next Subsection, we present the main steps of the micro-diagonalization method and refer to [14, 3, 9] for more details. For the sake of simplicity, the velocity c is supposed to be equal to 1, but our work can be easily reproduced for any velocity.

2.1 The micro-diagonalization method applied to the wave equation

We tackle the construction of ABCs by applying a factorization theorem proposed by M.E. Taylor [24] to study the propagation of singularities of strictly hyperbolic systems. Because we want to build low-order conditions, we limit our work to the application of the first step of factorization. We are thus only dealing with the diagonalization of the principal symbol of the wave equation, according to the mathematical analysis in [3], which shows that the next steps necessarily involve differential operators with order higher than two.
The ABCs that we consider are derived from the micro-local approximation of the DtN operator related to the artificial surface Σ. We thus begin with rewriting the acoustic wave equation in a local coordinate system (r, s). The couple (r, s) describes a point in the neighborhood of Σ in such a way that $\Sigma = \{r = 0\}$. We use the same coordinate system as in [4] and the acoustic wave equation reads then as

$$\partial_t^2 u - \partial_r^2 u - \kappa_r \partial_r u - h^{-1}\partial_s \left(h^{-1}\partial_s u\right) = 0, \tag{3}$$

where κ is the curvature of Σ, $h = 1 + r\kappa(s)$ and $\kappa_r = h^{-1}\kappa$.
Next, to apply Taylor's method, we rewrite (3) as a first-order system. We thus introduce an auxiliary unknown v which satisfies $\partial_t v + \partial_r u = 0$ in a neighborhood of Σ and such that the field $\mathbf{U} = (v, u)$ is solution to the first-order system $\partial_r \mathbf{U} = L\mathbf{U}$. The entries of L are first-order pseudo-differential operators and $\sigma(L) = \mathcal{L} = \mathcal{L}_1 + \mathcal{L}_0$ is given by

$$\mathcal{L}_1 = \begin{pmatrix} 0 & -\frac{h^{-2}\xi^2 - \omega^2}{i\omega} \\ -i\omega & 0 \end{pmatrix} \in S^1 \quad \text{and} \quad \mathcal{L}_0 = \begin{pmatrix} -\kappa_r & -\frac{h^{-3}\partial_s(h)\xi}{\omega} \\ 0 & 0 \end{pmatrix} \in S^0,$$

where ξ and ω are the dual variables respectively associated to s and t. We use standard notations such as $\sigma(L)$ for the symbol of L. Thereafter, as in [24], we note more concisely by S^m the symbol class $S^m_{1,0}$ introduced by [19]. We also denote by $\tau_{-m}(\sigma(L))$ the truncation at the order m of the asymptotic expansion of the symbol $\sigma(L)$.
Let λ_1 denote the symbol $\lambda_1 = \left(h^{-2}\xi^2 - \omega^2\right)^{1/2}$. Then, when $\lambda_1 \neq 0$, the principal symbol of $\mathcal{L}$ admits two single eigenvalues λ_1 and $-\lambda_1$. When $h^{-2}\xi^2 - \omega^2 > 0$, (ω, ξ) belongs to the elliptic region and λ_1 is real. When $h^{-2}\xi^2 - \omega^2 < 0$, λ_1 is imaginary and corresponds to propagating modes for which (ω, ξ) covers the hyperbolic region. Following [3, 14], we introduce

$$\mathcal{V}_0 = \frac{1}{\sqrt{2}} \begin{pmatrix} \frac{i\omega}{\lambda_1} & 1 \\ 1 & -\frac{\lambda_1}{i\omega} \end{pmatrix}, \text{ so that } \mathcal{V}_0 \mathcal{L}_1 \mathcal{V}_0^{-1} = \begin{pmatrix} \lambda_1 & 0 \\ 0 & -\lambda_1 \end{pmatrix} = \mathcal{M}_1.$$

Now, a first-order ABC can be derived from the approximation and the localization of the global boundary condition

$$\left[(I + K_{-1})\, V_0 \mathbf{U}\right]_2 = 0 \text{ on } \Sigma, \tag{4}$$

where $[\cdot]_2$ represents the second component of the vector, V_0 is the Fourier Integral Operator (FIO) with symbol $\mathcal{V}_0$ and K_{-1} is a regularizing operator of order -1.
According to [24], the principal symbol of K_{-1} is fixed by imposing that
$W_1 = (I + K_{-1})\, V_0 U$ is solution to $\partial_r W_1 = (\Lambda_1 + \Lambda_0)\, W_1 + R_{-1} W_1$, where Λ_1 is the FIO with the symbol $\mathcal{M}_1$ and Λ_0 is a diagonal FIO also (see [3, 23]). Indeed, by setting (4) on Σ, we impose that the in-going component of W_1 vanishes on Σ. By this way, we select only the out-going component of W_1 and an ABC is obtained after localizing (4).
Therefore, the principal symbol of K_{-1}, denoted by $\mathcal{K}_{-1}$, is determined by the condition : Λ_0 is a diagonal operator. Observe that this condition fixes only the off-diagonal entries of $\mathcal{K}_{-1}$ (see [3]) and most of the works using this approach consider

$$\mathcal{K}_{-1} = \begin{pmatrix} 0 & -\frac{i\kappa\omega^3}{4\lambda_1^4} \\ -\frac{i\kappa\omega}{4\lambda_1^2} & 0 \end{pmatrix}. \tag{5}$$

Then, after using a truncated Taylor expansion of λ_1 in the hyperbolic region with $\omega^2 \gg h^{-2}\xi^2$, (4) gives rise to $\partial_t u + \partial_n u + \frac{\kappa}{2} u = 0$ on Σ. The resulting condition involves differential operators but it should be called micro-differential since it is justified in the propagating cone $\omega^2 \gg h^{-2}\xi^2$. This condition is widely used in case of curved surfaces. We will refer to this condition as the C-ABC for "Curvature ABC".
Now, it might be interesting to see how the condition changes by considering non-zero diagonal entries for $\mathcal{K}_{-1}$. We address this issue in the following Subsection.

2.2 A new family of ABCs

The idea of modifying $\mathcal{K}_{-1}$ by introducing non-zero diagonal entries has been formerly applied in [8] for the 2D Maxwell system, but only from a theoretical point of view. To the best of our

knowledge, the numerical impact of using these conditions has never been investigated. Herein, we propose to modify $\mathcal{K}_{-1}$ as follows

$$\mathcal{K}_{-1} = \begin{pmatrix} 0 & -\dfrac{i\kappa\omega^3}{4\lambda_1^4} \\ -\dfrac{i\kappa\omega}{4\lambda_1^2} & \dfrac{\gamma(s)}{\lambda_1} \end{pmatrix}, \tag{6}$$

where γ is a parameter depending only on the curvilinear abscissa s. Let us note that we do not change the first diagonal entry since it is not involved in condition (4). We then get

Theorem 2.1 *A family of first-order condition is given by*

$$\partial_t \left(\partial_n u + \partial_t u\right) = \left(\frac{\kappa}{4} - \gamma\right) \partial_n u - \left(\frac{\kappa}{4} + \gamma\right) \partial_t u \text{ on } \Sigma, \tag{7}$$

where γ is a regular function defined on Σ.

▷ Proof : We recall that the first-order boundary condition is given by $\left[\left(I + K_{-1}\right) V_0 \mathbf{U}\right]_2 = 0$ on Σ. The symbol of the corresponding operator reads as

$$\sigma\left(\left(I + K_{-1}\right) V_0\right) = \left(\mathcal{I}_2 + \mathcal{K}_{-1}\right) \mathcal{V}_0 + \mathcal{R}_{-2},$$

where $\mathcal{R}_{-2} \in S^{-2}$. Therefore, the truncation of $\sigma\left(\left(I + K_{-1}\right) V_0\right)$ in S^{-1} is given by

$$\begin{aligned} \tau_{-1}\left(\left(I + K_{-1}\right) V_0\right) &= \left(\mathcal{I}_2 + \mathcal{K}_{-1}\right) \mathcal{V}_0 \\ &= \frac{1}{\sqrt{2}} \begin{pmatrix} \dfrac{i\omega}{\lambda_1} - \dfrac{i\kappa\omega^3}{4\lambda_1^4} & 1 + \dfrac{\kappa\omega^2}{4\lambda_1^3} \\ \dfrac{\kappa\omega^2}{4\lambda_1^3} + 1 + \dfrac{\gamma(s)}{\lambda_1} & -\dfrac{i\kappa\omega}{4\lambda_1^2} - \dfrac{\lambda_1}{i\omega} - \dfrac{\gamma(s)}{i\omega} \end{pmatrix}. \end{aligned} \tag{8}$$

Using a first-order Taylor expansion for $\omega \gg h^{-1}\xi$, we then obtain

$$\tau_{-1}\left(\mathcal{I}_2 + \mathcal{K}_{-1}\right) \mathcal{V}_0 = \frac{1}{\sqrt{2}} \begin{pmatrix} 1 - \dfrac{i\kappa}{4\omega} & 1 + \dfrac{i\kappa}{4\omega} \\ 1 + \dfrac{i\kappa}{4\omega} + \dfrac{\gamma}{i\omega} & \dfrac{i\kappa}{4\omega} - 1 - \dfrac{\gamma}{i\omega} \end{pmatrix}. \tag{9}$$

Since $\mathbf{U} = (v, u)$, with $\partial_t v + \partial_n u = 0$ on Σ, is supposed to satisfy (4), we get

$$\partial_t \left(\partial_n u + \partial_t u\right) = \left(\frac{\kappa}{4} - \gamma\right) \partial_n u - \left(\frac{\kappa}{4} + \gamma\right) \partial_t u \text{ on } \Sigma,$$

◁

When $\gamma = \frac{\kappa}{4}$, we have

$$\tau_{-1}\left(\mathcal{I}_2 + \mathcal{K}_{-1}\right) \mathcal{V}_0 = \frac{1}{\sqrt{2}} \begin{pmatrix} 1 - \dfrac{i\kappa}{4\omega} & 1 + \dfrac{i\kappa}{4\omega} \\ 1 & \dfrac{i\kappa}{2\omega} - 1 \end{pmatrix}$$

and the boundary condition reduces to $\partial_n u + \partial_t u + \dfrac{\kappa}{2} u = 0$ on Σ. We thus recover the C-ABC for the particular choice $\gamma = \frac{\kappa}{4}$.

Before we focus on the property (3) defined in the introduction to this paper, we wish to go back over the construction method that we used. Indeed it might seem more natural to apply the Nirenberg factorization technique [22] in particular because it is well-suited for scalar equations like the acoustic wave equation. But, if we set the same degree of approximations on the symbols, this process will only lead to the construction of the C-ABC, whereas the one used herein leads to a family of ABCs. Our approach is thus more productive for the same fixed level of approximation of the symbol and the same amount of computations.

3 Mathematical analysis

We consider the solution of the scattering by a sound soft obstacle when using the family of ABCs that have been constructed in the previous section. The corresponding BVP reads as : find u solution to

$$\begin{aligned}
&\partial_t^2 u - \Delta u = 0 && \text{in } \Omega \times (0,+\infty)\,;\\
&u(0,x) = u_0(x),\ \partial_t u(0,x) = u_1(x) && \text{in } \Omega;\\
&u = 0 && \text{on } \Gamma \times (0,+\infty)\,;\\
&\partial_t\left(\partial_n u + \partial_t u\right) = \left(\frac{\kappa}{4} - \gamma\right)\partial_n u - \left(\frac{\kappa}{4} + \gamma\right)\partial_t u && \text{on } \Sigma \times (0,+\infty)\,.
\end{aligned} \tag{10}$$

Now, we aim at numerically solving (10) and, as a matter of fact, the condition on Σ is not easy to include in a variational formulation of the acoustic wave equation. Indeed, the boundary condition on Σ steps in the numerical scheme through the formal integrand $\int_\Sigma \partial_n u \varphi d\sigma$, where φ is a test-function. Hence, to include the boundary condition on Σ requires to multiply by the pseudo-differential operator $\left(\partial_t + \gamma - \frac{\kappa}{4}\right)^{-1}$. The sparsity of the finite element matrix is thus violated. This is why we propose an equivalent formulation involving an auxiliary unknown ψ defined on Σ. It is

$$\begin{aligned}
&\partial_t^2 u - \Delta u = 0 && \text{in } \Omega \times (0,+\infty)\,;\\
&\left(\partial_t - \frac{\kappa}{4} + \gamma\right)\psi = \partial_t u, && \text{on } \Sigma \times (0,+\infty)\,;\\
&\partial_n u + \partial_t u + \frac{\kappa}{2}\psi = 0 && \text{on } \Sigma \times (0,+\infty)\,;\\
&u = 0 && \text{on } \Gamma \times (0,+\infty)\,;\\
&u(0,x) = u_0(x),\ \partial_t u(0,x) = u_1(x) && \text{in } \Omega;\\
&\psi(0,x) = \psi_0(x) && \text{on } \Sigma.
\end{aligned} \tag{11}$$

The initial datum ψ_0 is given as a function of u_0 and u_1 on Σ satisfying the compatibility relation $\partial_n u_0 + u_1 + \frac{\kappa}{2}\psi_0 = 0$ on Σ.

Remark 3.1 *Observe that in the context of an ABC method, Σ must be chosen in such a way that the supports of u_0 and u_1 are fully embedded inside Ω. In that case, we thus have $\psi(x,0) = \psi_0 = 0$ on Σ.*

In the following, the function κ always denotes the curvature of Σ and γ is a regular parameter defined on Σ. The domain Ω is a bounded domain and its boundary $\partial\Omega = \Gamma \cup \Sigma$ is assumed to be regular, with $\Gamma \cap \Sigma = \varnothing$ (see Fig. 1).

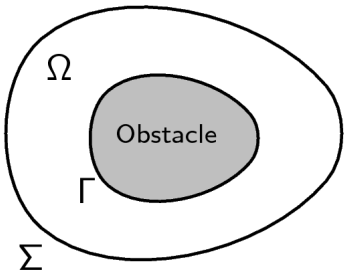

Figure 1: Studied domain

To simplify the presentation of the theoretical results, we assume that κ and γ check the following condition

$$\kappa \in L^\infty(\Sigma) \text{ and } \gamma(x) > \frac{\kappa(x)}{4}, \forall x \in \Sigma. \tag{12}$$

We do not consider the case $\gamma = \frac{\kappa}{4}$ because it corresponds to a particular case where the ABC is the C-ABC. Then, the BVP (10) can be studied directly, without considering the auxiliary problem (11). We thus make do with setting existing results that are proved in [11].
We first transform (11) in a first order system in time. We introduce an auxiliary unknown v defined by $v = \partial_t u$. The vector $\mathbf{U} = (u, v, \psi)$ is thus solution to

$$\frac{dU}{dt} = AU,\ A = \begin{pmatrix} 0 & Id & 0 \\ \Delta & 0 & 0 \\ 0 & 1 & \frac{\kappa}{4} - \gamma \end{pmatrix} \tag{13}$$

with the boundary conditions $u = 0$ on $\Gamma \times (0, +\infty)$ and $\partial_n u + \partial_t u + \frac{\kappa}{2}\psi = 0$ on $\Sigma \times (0, +\infty)$.

In the following, we will concentrate on formulation (13) and we will interest ourselves on its solution in suitable Hilbert spaces. As usual, H^s denotes the Sobolev space of order $s \in \mathbb{R}$.
Let us first introduce H as the product space defined by $H = H^1_\Gamma(\Omega) \times L^2(\Omega) \times L^2(\Sigma)$, where $H^1_\Gamma(\Omega) = \{h_1 \in H^1(\Omega),\ h_1 = 0 \text{ on } \Gamma\}$. We equip H with the Hilbertian graph norm

$$\| (h_1, h_2, h_3) \|_H = \left(\|h_1\|^2_{L^2(\Omega)} + \|\nabla h_1\|^2_{L^2(\Omega)} + \|h_2\|^2_{L^2(\Omega)} + \|h_3\|^2_{L^2(\Sigma)} \right)^{1/2}.$$

Let V be the product space defined by

$$V = \{(v_1, v_2, \varphi) \in H, A(v_1, v_2, \varphi) \in H, \partial_n v_1 + v_2 + \frac{\kappa}{2}\varphi = 0 \text{ on } \Sigma\}.$$

The space V corresponds to the domain of A. By enforcing $A(v_1, v_2, \varphi) \in H$, the regularity of the unknown is improved. Indeed, we then have $v_2 \in H^1_\Gamma(\Omega)$ and $\Delta v_1 \in L^2(\Omega)$. Then, $v_2 \in H^1_\Gamma(\Omega)$ implies that $v_{2|_\Sigma}$ is defined in $H^{1/2}(\Sigma)$ and $\Delta v_1 \in L^2(\Omega)$ implies that $\partial_n v_{1|_\Sigma} \in H^{-1/2}(\Sigma)$, knowing that $v_1 \in H^1(\Omega)$. Moreover, the relation $\partial_n v_1 + v_2 + \frac{\kappa}{2}\varphi = 0$ on Σ improves the regularity of $\partial_n v_{1|_\Sigma}$ since $v_2 + \frac{\kappa}{2}\varphi \in L^2(\Sigma)$. Hence, to sum up, we have

$$\begin{aligned} V = \quad & \{(v_1, v_2, \varphi) \in H,\ \Delta v_1 \in L^2(\Omega),\ v_2 \in H^1_\Gamma(\Omega),\ \partial_n v_{1|_\Sigma} \in L^2(\Sigma), \\ & \partial_n v_1 + v_2 + \frac{\kappa}{2}\varphi = 0 \text{ on } \Sigma\}. \end{aligned}$$

We recall the Green formula we will use: for all $(u,v) \in H^1(\Omega) \times H^1(\Omega)$ such that $\Delta u \in L^2(\Omega)$, we have

$$\int_\Omega \Delta u v \, dx = -\int_\Omega \nabla u \cdot \nabla v \, dx + \langle \partial_n u, v \rangle_{H^{-1/2}(\partial\Omega), H^{1/2}(\partial\Omega)}. \tag{14}$$

Lemma 3.2 *Let κ be given in $L^\infty(\Sigma)$ and such that $\min_{x\in\Sigma} \kappa(x) = \kappa_0 > 0$. Then, for all $h \in H$, the quantity*

$$|||h||| = \left(\int_\Omega |\nabla h_1|^2 + |h_2|^2 \, dx + \int_\Sigma \frac{\kappa}{2} |h_3|^2 \, d\sigma \right)^{1/2}$$

is a norm on H equivalent to the norm $\|h\|_H$.

▷ Proof : It is well-known that $\|\nabla \cdot \|_{L^2(\Omega)}$ defines a norm on $H^1_\Gamma(\Omega)$ which is equivalent to the standard norm in $H^1(\Omega)$, as a consequence of the Poincaré inequality. Hence, since the curvature κ is supposed to be in $L^\infty(\Sigma)$ with $\min_{x\in\Sigma} \kappa(x) > 0$, it is straightforward that $|||\cdot|||$ defines a norm on H equivalent to the conventional norm $\|\cdot\|_H$. ◁

In the following, we denote by $(\ ,\ )$ the scalar product derived from the norm $|||\ |||$.

Lemma 3.3 *Let κ and γ be given such that (12) is checked. Then, for all $v \in V$, we have $(Av, v) \leqslant 0$.*

▷ Proof : Let $v = (v_1, v_2, \varphi)$ in V. By definition of A, $Av = \left(v_2, \Delta v_1, v_2 + \left(\frac{\kappa}{4} - \gamma\right)\varphi\right)$. Then, we have

$$(Av, v) = \int_\Omega \nabla v_2 \cdot \nabla v_1 \, dx + \int_\Omega \Delta v_1 v_2 \, dx + \int_\Sigma \frac{\kappa}{2} \left(v_2 + \left(\frac{\kappa}{4} - \gamma \right) \varphi \right) \varphi \, d\sigma.$$

Using the Green formula (14), we get

$$\begin{aligned}(Av, v) = \ & \int_\Omega \nabla v_2 \cdot \nabla v_1 \, dx - \int_\Omega \nabla v_2 \cdot \nabla v_1 \, dx + \int_\Sigma \partial_n v_1 v_2 \, d\sigma \\ & + \langle \partial_n v_1, \, v_2 \rangle_{H^{-1/2}(\Gamma), H^{1/2}(\Gamma)} + \int_\Sigma \frac{\kappa}{2} \left(v_2 + \left(\frac{\kappa}{4} - \gamma \right) \varphi \right) \varphi \, d\sigma.\end{aligned}$$

Moreover, in V, we have $v_{1|\Gamma} = v_{2|\Gamma} = 0$ and on Σ, $\partial_n v_1 = -v_2 - \frac{\kappa}{2}\varphi$. Hence,

$$(Av, v) = -\int_\Sigma |v_2|^2 \, d\sigma - \int_\Sigma \frac{\kappa}{2} \varphi v_2 \, d\sigma + \int_\Sigma \frac{\kappa}{2} \varphi v_2 \, d\sigma + \int_\Sigma \frac{\kappa}{2} \left(\frac{\kappa}{4} - \gamma \right) |\varphi|^2 \, d\sigma.$$

Now, since $\frac{\kappa}{2}\left(\frac{\kappa}{4} - \gamma\right) \leqslant 0$ on Σ, we get that for all v in V

$$(Av, v) = -\int_\Sigma |v_2|^2 \, d\sigma + \int_\Sigma \frac{\kappa}{2} \left(\frac{\kappa}{4} - \gamma \right) |\varphi|^2 \, d\sigma \leqslant 0,$$

which completes the proof of Lemma 3.3. ◁

Lemma 3.4 *The operator A, with domain V, is maximal.*

▷ Proof : Given $f = (f_1, f_2, f_3)$ in H, we consider the following mixed problem: find $v \in V$ such that $(A - I)\, v = f$.
We thus seek $v = (v_1, v_2, \varphi) \in V$ such that

$$\begin{array}{ll} v_2 - v_1 = f_1 & \text{in } \Omega; \\ \Delta v_1 - v_2 = f_2 & \text{in } \Omega; \\ v_2 + \left(\dfrac{\kappa}{4} - \gamma - 1\right)\varphi = f_3, \partial_n v_1 + v_2 + \dfrac{\kappa}{2}\varphi = 0 & \text{on } \Sigma; \\ v_1 = 0 & \text{on } \Gamma; \end{array} \tag{15}$$

Assume now that the problem (15) has a solution in V. Then, by removing v_2 thanks to the first equation, $v_2 = f_1 + v_1$, in Ω, and φ, thanks to the third equation, $\varphi = \frac{f_3 - f_1 - v_1}{\frac{\kappa}{4} - \gamma - 1}$, we obtain that v_1 is solution to the boundary-value problem

$$\begin{array}{ll} -\Delta v_1 + v_1 = \tilde{f} & \text{in } \Omega; \\ v_1 = 0 & \text{on } \Gamma; \\ \partial_n v_1 + \alpha v_1 = \tilde{g} & \text{on } \Sigma. \end{array} \tag{16}$$

with $\tilde{f} := -\left(f_2 + f_1\right)$ in $L^2(\Omega)$, $\alpha = 1 + \frac{\kappa}{2\left(1+\gamma-\frac{\kappa}{4}\right)} > 0$ and

$$\tilde{g} := -\left(1 + \frac{\kappa}{2\left(1+\gamma-\frac{\kappa}{4}\right)}\right) f_1 + \frac{\kappa}{2\left(1+\gamma-\frac{\kappa}{4}\right)} f_3 \text{ in } L^2(\Sigma).$$

It is obvious that, since $\kappa \in L^\infty(\Sigma)$ and $\alpha > 0$ by hypothesis, the functional

$$|v|_{1,\alpha} = \left(\|v\|^2_{H^1(\Omega)} + \int_\Sigma \alpha |v|^2 d\sigma\right)^{1/2}$$

defines a norm in $H^1(\Omega)$ which is equivalent to the standard norm $\|\,\|_{H^1(\Omega)}$. Let $\mathcal{T}\left(\overline{\Omega}\right)$ be the space of test functions defined by $\mathcal{T}\left(\overline{\Omega}\right) = \{\phi \in \mathcal{D}\left(\overline{\Omega}\right),\, \phi_{|\Gamma} = 0\}$. It is dense in $H^1_\Gamma(\Omega)$ and if we assume that the problem (16) has a regular solution, we have

$$\forall \phi \in \mathcal{T}\left(\overline{\Omega}\right), -\int_\Omega \Delta v_1 \phi\, dx + \int_\Omega v_1 \phi\, dx = \int_\Omega \tilde{f}\phi\, dx.$$

By using the Green formula (14), we get $\forall \phi \in \mathcal{T}\left(\overline{\Omega}\right)$,

$$\int_\Omega \nabla v_1 \nabla \phi\, dx - \langle \partial_n v_1,\, \phi \rangle_{H^{-1/2}(\partial\Omega), H^{1/2}(\partial\Omega)} + \int_\Omega v_1 \phi\, dx = \int_\Omega \tilde{f}\phi\, dx.$$

Moreover, $\phi_{|\Gamma} = 0$. Therefore,

$$\forall \phi \in \mathcal{T}\left(\overline{\Omega}\right), \int_\Omega \nabla v_1 \nabla \phi\, dx - \int_\Sigma \partial_n v_1 \phi\, d\sigma + \int_\Omega v_1 \phi\, dx = \int_\Omega \tilde{f}\phi\, dx.$$

Then, by using that $\partial_n v_1 = \tilde{g} - \alpha v_1$ on Σ, we obtain

$$\forall \phi \in \mathcal{T}\left(\overline{\Omega}\right), \int_\Omega \nabla v_1 \nabla \phi\, dx + \int_\Sigma \alpha v_1 \phi\, d\sigma + \int_\Omega v_1 \phi\, dx = \int_\Omega \tilde{f}\phi\, dx + \int_\Sigma \tilde{g}\phi\, d\sigma. \tag{17}$$

Let $a(\cdot,\cdot)$ be the bilinear form defined by $a(v_1, \phi) = \int_\Omega \nabla v_1 \nabla \phi\, dx + \int_\Sigma \alpha v_1 \phi\, d\sigma + \int_\Omega v_1 \phi\, dx$. It is obvious that $a(\cdot,\cdot)$ is continuous on $H^1_\Gamma(\Omega) \times H^1_\Gamma(\Omega)$ and $H^1_\Gamma(\Omega)$-coercive, since $a(v_1, \phi)$ corresponds exactly to the scalar product associated to the norm $|\cdot|_{1,\alpha}$. Let $l(\cdot)$ be the linear form defined by $l(\phi) = \int_\Omega \tilde{f}\phi\, dx + \int_\Sigma \tilde{g}\phi\, d\sigma$. Since the pair $(\tilde{f}, \tilde{g})$ belongs to $L^2(\Omega) \times L^2(\Sigma)$,

$l(\cdot)$ is continuous in $H^1_\Gamma(\Omega)$.
Then, according to the fact that $\mathcal{T}\left(\overline{\Omega}\right)$ is dense in $H^1_\Gamma(\Omega)$, the formulation (17) can be extended to $H^1_\Gamma(\Omega)$: $\forall \phi \in H^1_\Gamma(\Omega)$, $a(v_1,\phi) = l(\phi)$ and, according to Lax-Milgram theorem, this problem has a unique solution v_1 in $H^1_\Gamma(\Omega)$. In particular,

$$\forall \phi \in \mathcal{D}(\Omega) \subset H^1_\Gamma(\Omega),\ \int_\Omega \nabla v_1 \nabla \phi\, dx + \int_\Omega v_1 \phi\, dx = \int_\Omega \tilde{f}\phi\, dx.$$

We then deduce that $\forall \phi \in \mathcal{D}(\Omega)$, $\langle v_1 - \Delta v_1 - \tilde{f}, \phi\rangle = 0$, where $\langle\ ,\ \rangle$ denotes the duality pairing between $\mathcal{D}'(\Omega)$ and $\mathcal{D}(\Omega)$, and we thus obtain $v_1 - \Delta v_1 = \tilde{f}$ in $\mathcal{D}'(\Omega)$.
This identity allows us to give a sense to Δv_1 in $L^2(\Omega)$. Therefore, $\partial_n v_{1|_{\partial\Omega}} \in H^{-1/2}(\partial\Omega)$ and we also have

$$\forall \phi \in \mathcal{T}\left(\overline{\Omega}\right),\ \int_\Omega \nabla v_1 \nabla \phi\, dx + \int_\Sigma \alpha v_1 \phi\, d\sigma + \int_\Omega v_1 \phi\, dx = \int_\Omega \tilde{f}\phi\, dx + \int_\Sigma \tilde{g}\phi\, d\sigma.$$

Using the Green formula (14), we get, $\forall \phi \in \mathcal{T}\left(\overline{\Omega}\right)$:

$$-\int_\Omega \Delta v_1 \phi\, dx\ + \langle \partial_n v_1, \phi\rangle_{H^{-1/2}(\partial\Omega),H^{1/2}(\partial\Omega)} + \int_\Sigma \alpha v_1 \phi\, d\sigma + \int_\Omega v_1 \phi\, dx =$$
$$\int_\Omega \tilde{f}\phi\, dx + \int_\Sigma \tilde{g}\phi\, d\sigma,$$

i.e., $\forall \phi \in \mathcal{T}\left(\overline{\Omega}\right)$, $\langle \partial_n v_1, \phi\rangle_{H^{-1/2}(\partial\Omega),H^{1/2}(\partial\Omega)} + \int_\Sigma \alpha v_1 \phi\, d\sigma = \int_\Sigma \tilde{g}\phi\, d\sigma$.
Now, we have $\phi_{|\Gamma} = 0$, which implies that

$$\langle \partial_n v_1 + \left(1 + \frac{\kappa}{2\left(1+\gamma-\frac{\kappa}{4}\right)}\right) v_1 - \tilde{g}, \phi\rangle_{H^{-1/2}(\Sigma),H^{1/2}(\Sigma)} = 0,$$

and we then have $\partial_n v_1 + \left(1 + \dfrac{\kappa}{2\left(1+\gamma-\frac{\kappa}{4}\right)}\right) v_1 = \tilde{g}$ on Σ.
The existence of v_1 as a solution to (16) is thus proved. Next, since v_1 and f_1 are in $H^1(\Omega)$, we deduce the existence of $v_2 = f_1 + v_1$ in $H^1(\Omega)$. Moreover since $v_{2|_\Sigma}$ and f_3 are in $L^2(\Sigma)$, $\varphi = \dfrac{f_3 - f_1 - v_1}{\frac{\kappa}{4} - \gamma - 1}$ exists in $L^2(\Sigma)$.
To complete the proof, we have to check that $(v_1, v_2, \varphi) \in V$, which is obvious, using the relations $v_2 = f_1 + v_1$ in Ω and $\alpha\varphi = f_3 - v_2$ on Σ and that $f_1 \in H^1_\Gamma(\Omega)$ and $f_3 \in L^2(\Sigma)$. $\lhd$

We are now willing to set the main result of this section:

Theorem 3.5 *Let $(u_0, u_1, \varphi_0) \in V$. The problem (11) admits a unique solution u such that $(u,\ \partial_t u,\ \varphi) \in C^1([0,+\infty[; V) \cap C^0([0,+\infty[; H)$.*

$\rhd$ Proof : The two previous lemmas show that the operator A is a maximal dissipative operator in its domain V. According to the Hille-Yosida theorem [20], the problem (11) has one and only one solution $\mathbf{U} = (u,\ v,\ \psi)$ such that $(u,\ v,\ \psi) \in C^1([0,+\infty[; V) \cap C^0([0,+\infty[; H)$. $\lhd$

Remark 3.6 *A is thus the infinitesimal generator of a semi-group of contraction $Z(t)$. We can thus define a finite energy solution of (11) with initial data (u_0, u_1, ψ_0) in H only. In that case, $(u,\ v,\ \psi) = Z(t)(u_0, u_1, \psi_0) \in C^1([0,+\infty[; V) \cap C^0([0,+\infty[; H)$.*

When $\gamma = \frac{\kappa}{4}$, we have [11] :

Theorem 3.7 *Let* $(u_0, u_1) \in W_1$ *with*

$$W_1 = \left\{(u,v) \in H^1(\Omega) \times H^1(\Omega),\ \Delta u \in L^2(\Omega),\ \partial_n u + v + \frac{\kappa}{2}u = 0 \text{ on } \Sigma\right\}.$$

Then the problem (10) admits a unique solution u *such that*

$$(u,\ \partial_t u,\ \varphi) \in C^1([0,+\infty[; W_1) \cap C^0([0,+\infty[; W_0), \tag{18}$$

where $W_0 = H^1_\Gamma(\Omega) \times L^2(\Omega)$.

We have established that the problem is well-posed if $\kappa > 0$ and $\gamma \geqslant \frac{\kappa}{4}$. The problem admits thus a solution when the external boundary Σ is convex. In the framework of ABCs, this is not restrictive since Σ is chosen by the engineer. Nevertheless, the well-posedness can also be obtained without any assumption on κ and γ, except suitable regularity hypotheses. Indeed, by multiplying u by $e^{-\delta t}$ with $\delta > \max(0, \max\limits_{x\in\Sigma} \frac{\kappa(x)}{4} - \gamma(x), -\min\limits_{x\in\Sigma} \frac{\kappa(x)}{4} + \gamma(x))$, we get an auxiliary and equivalent problem for which a proof of the existence and uniqueness is achieved for any κ and γ. We refer to [9] for a detailed proof for the general case. Let us also mention that the well-posedness of the initial formulation (10) has been established in [9] and the case of a Neumann boundary condition is also considered. Herein, we decided to select a set of suitable values for κ and γ that allows to consider a large rank of applications and that provides simplified but informative proofs.

Regarding applications, it is interesting to consider the case where the acoustic wave is generated by a source field S. Then the initial data vanish and, in practice, S is compactly supported in a time interval $[0,T]$. We can apply the Hille-Yosida theory providing $S \in C^1([0,+\infty[, H)$. The wave field can then be written thanks to the Duhamel formula in $[0,T]$ and for $t \geqslant T$, the previous study is still valid by considering the solution $(u, \partial_t u, \psi)$ at $t = T$ as an initial wave field.

4 Long-term behavior

The results of Section 3 can be enhanced by introducing the functional defined on H by

$$\mathcal{E}(h_1,h_2,h_3) = \frac{1}{2}\int_\Omega \left(|\nabla h_1|^2 + |h_2|^2\right) dx + \frac{1}{2}\int_\Sigma \frac{\kappa}{2}|h_3|^2 d\sigma. \tag{19}$$

If $\kappa(x) \geqslant 0$ for all $x \in \Sigma$, $\mathcal{E}$ is positive on H and if $\kappa > 0$ on Σ, $\mathcal{E}^{1/2}$ is obviously a norm in H equivalent to the norm $|||\ |||$, according to Lemma 3.2. Then, $\mathcal{E}(u, \partial_t u, \psi)$ defines an energy on H. Moreover,

Lemma 4.1 *For all* $(u_0, u_1, \psi_0) \in V$, $t \longmapsto \mathcal{E}(u, \partial_t u, \psi)$ *is differentiable and is decreasing under the condition (12):* $\gamma(x) \geqslant \dfrac{\kappa(x)}{4}, \forall x \in \Sigma$.

▷ Proof : In the previous section, we have seen that if the initial conditions (u_0, u_1, ψ_0) are in V, $\mathcal{E}(u, \partial_t u, \psi) \in C^1([0,+\infty[)$. Moreover,

$$\frac{d}{dt}\mathcal{E}(u, \partial_t u, \psi) = \int_\Omega \nabla(\partial_t u) \cdot \nabla u\, dx + \int_\Omega \partial_t u \partial_t^2 u\, dx + \int_\Sigma \frac{\kappa}{2}\psi \partial_t \psi\, d\sigma. \tag{20}$$

Using the Green formula (14) and the relation $\partial_t^2 u = \Delta u$ in Ω, we obtain

$$\frac{d}{dt}\mathcal{E}(u,\partial_t u,\psi) = -\int_\Omega \partial_t u \Delta u\, dx + \int_{\partial\Omega} \partial_n u \partial_t u\, d\sigma + \int_\Omega \partial_t u \Delta u\, dx + \int_\Sigma \frac{\kappa}{2}\psi\partial_t\psi\, d\sigma.$$

Since $\partial_t u_{|\Gamma} = 0$ and $\partial_n u = -\partial_t u - \frac{\kappa}{2}\psi$ on Σ,

$$\frac{d}{dt}\mathcal{E}(u,\partial_t u,\psi) = -\int_\Sigma |\partial_t u|^2 d\sigma - \int_\Sigma \frac{\kappa}{2}\psi\partial_t u d\sigma.$$

At last, since $\partial_t\psi = \partial_t u - \left(\gamma - \frac{\kappa}{4}\right)\psi$, we get

$$\frac{d}{dt}\mathcal{E}(u,\partial_t u,\psi) = -\left[\int_\Sigma \frac{\kappa}{2}\left(\gamma - \frac{\kappa}{4}\right)|\psi|^2\, d\sigma + \int_\Sigma |\partial_t u|^2\, d\sigma\right].$$

which implies that $\frac{d}{dt}\mathcal{E}(u,\partial_t u,\psi) \leqslant 0$, if $\gamma \geqslant \frac{\kappa}{4}$ and $\kappa \geqslant 0$, and completes the proof of Lemma 4.1. ◁

Remark 4.2 *Lemma 4.1 has been proved in [11, 7] when* $\gamma = \frac{\kappa}{4}$.

In the following, we will assume that $\psi_0 = 0$ on Σ, without being restrictive on the application domain of our work. Indeed, as it was previously discussed in Remark 3.1, ψ_0 must vanish on Σ in the framework of ABCs methods.

Theorem 4.3 *Under (12), for all* $(u_0, u_1, 0) \in V$, $\lim_{t\to+\infty} \mathcal{E}(u,\partial_t u,\psi) = 0$.

▷ Proof : We have already seen that A is the generator of a continuous contraction semi-group $Z(t)$. As it is sufficient to prove the theorem on a dense subspace of $V = D(A)$, we consider the initial data $(u_0, u_1, 0)$ in $D(A^2)$, where

$$D(A^2) = \{(v_1, v_2, \psi) \in V, A(v_1, v_2, \psi) \in V\}$$

is equipped with the graph norm

$$\|(v_1, v_2, \psi)\|_{D(A^2)} = \|(v_1, v_2, \psi)\|_V + \|A(v_1, v_2, \psi)\|_V + \|A^2(v_1, v_2, \psi)\|_V.$$

For any solution to (11), we have

$$\begin{aligned}\|(u,\partial_t u,\psi)\|_{D(A^2)} &= \|Z(t)(u_0,u_1,0)\|_{D(A^2)}\\ &= \|Z(t)(u_0,u_1,0)\|_V + \|A(Z(t)(u_0,u_1,0))\|_V\\ &+\|A^2(Z(t)(u_0,u_1,0))\|_V.\end{aligned}$$

As A, A^2 and $Z(t)$ are commuting on $D(A^2)$,

$$\begin{aligned}\|(u,\partial_t u,\psi)\|_{D(A^2)} &= \|Z(t)(u_0,u_1,0)\|_V + \|Z(t)A(u_0,u_1,0)\|_V\\ &+\|Z(t)A^2(u_0,u_1,0)\|_V.\end{aligned}$$

Since $Z(t)$ is continuous in V, we easily deduce that there exists a positive constant C such that $\|(u,\partial_t u,\psi)\|_{D(A^2)} \leqslant C\|(u_0,u_1,0)\|_{D(A^2)}$. We thus have a bounded sequence of solutions in $D(A^2)$ which implies that we can extract a subsequence denoted by $Z(t_k)(u_0,u_1,0)$ which weakly converges to $(u_\infty, v_\infty, \psi_\infty)$ in $D(A^2)$. Now, let us denote by $(u(t_k), v(t_k))$ the sequence

that is converging to (u_∞, v_∞). By definition of $D(A^2)$, $(u(t_k), v(t_k))$ is bounded in $H^{3/2}(\Omega) \times H^{3/2}(\Omega)$ and $\Delta u(t_k)$ is bounded in $H^1(\Omega)$. Indeed, any (u, v) in $D(A^2)$ satisfies

$$u \in H^1(\Omega),\ \Delta u \in H^1(\Omega),\ u = 0 \text{ on } \Gamma,\ \partial_n u_{|\Sigma} \in L^2(\Sigma),$$
$$v \in H^1(\Omega),\ \Delta v \in H^1(\Omega),\ v = 0 \text{ on } \Gamma,\ \partial_n v_{|\Sigma} \in L^2(\Sigma),$$

and, since Ω is regular,

$$\left\{w \in H^1(\Omega),\ \Delta w \in H^1(\Omega),\ w = 0 \text{ on } \Gamma,\ \partial_n w_{|\Sigma} \in L^2(\Sigma)\right\} \subset H^{3/2}(\Omega). \tag{21}$$

We can thus deduce that $(u(t_k), v(t_k))$ strongly converges to (u_∞, v_∞) in $H^1(\Omega) \times H^1(\Omega)$ according to the compact injection of $H^{3/2}(\Omega)$ into $H^1(\Omega)$. Moreover, $\Delta u(t_k)$ strongly converges in $L^2(\Omega)$ since it is bounded in $H^1(\Omega)$. Since $\Delta u(t_k)$ converges to Δu_∞ in $\mathcal{D}'(\Omega)$, we have that $\Delta u(t_k)$ strongly converges to Δu_∞ in $L^2(\Omega)$, according to the limit uniqueness.
We then deduce that $\partial_n u(t_k)_{|\Sigma}$ strongly converges to $\partial_n u_{\infty|\Sigma}$ in $H^{-1/2}(\Sigma)$ and that $v(t_k)_{|\Sigma}$ strongly converges to $v_{\infty|\Sigma}$ in $H^{1/2}(\Sigma)$. This implies that $\psi(t_k)$ strongly converges to ψ_∞ in $H^{-1/2}(\Sigma)$.

Nevertheless, this convergence result is not sufficient to prove that $(u(t_k), v(t_k), \psi(t_k))$ strongly converges to $(u_\infty, v_\infty, \psi_\infty)$ in V, because $\psi(t_k)$ should strongly converge in $L^2(\Sigma)$. That is why we go back to the equation satisfied by $\psi(t_k)$. By construction, ψ is solution to: $\partial_t \psi + \left(\gamma - \frac{\kappa}{4}\right)\psi = v$ on $\Sigma \times (0, +\infty)$ and $\psi(0, x) = 0$ on Σ. Then, according to the Duhamel formula, we have $\psi(t, x) = \displaystyle\int_0^t e^{\left(\gamma - \frac{\kappa}{4}\right)(s-t)} v(s, x) ds$.

We know that v is bounded in $H^{1/2}(\Sigma)$. Hence, if $\alpha_{\min} = \min\limits_{x \in \Sigma}\left(\gamma - \frac{\kappa}{4}\right)$, we have: for any $\xi \in H^{-1/2}(\Sigma)$,

$$\begin{aligned}\langle \psi, \xi \rangle_{H^{1/2}(\Sigma), H^{-1/2}(\Sigma)} &= \Big\langle \int_0^t e^{\left(\gamma - \frac{\kappa}{4}\right)(s-t)} v ds, \xi \Big\rangle_{H^{1/2}(\Sigma), H^{-1/2}(\Sigma)} \\ &\leqslant \int_0^t e^{\alpha_{\min}(s-t)} \langle v, \xi \rangle_{H^{1/2}(\Sigma), H^{-1/2}(\Sigma)} ds\end{aligned}$$

according to the fact that $v(s)$ is uniformly bounded with respect to s. Thus we obtain

$$|\langle \psi, \xi \rangle_{H^{1/2}(\Sigma), H^{-1/2}(\Sigma)}| \leqslant \frac{1}{\alpha_{\min}} \|v\|_{H^{1/2}(\Sigma)} \|\xi\|_{H^{-1/2}(\Sigma)} (1 - e^{-\alpha_{\min} t})$$

which implies $\|\psi\|_{H^{1/2}(\Sigma)} \leqslant \frac{1}{\alpha_{\min}}(1 - e^{-\alpha_{\min} t})\|v\|_{H^{1/2}(\Sigma)}$.

Then, $\psi(t)$ is uniformly bounded in $H^{1/2}(\Sigma)$ and we can then deduce that $\psi(t_k)$ strongly converges to ψ_∞ in $L^2(\Sigma)$, as a consequence of the compact injection from $H^{1/2}(\Sigma)$ into $L^2(\Sigma)$. As a conclusion, $(u(t_k), v(t_k), \psi(t_k))$ strongly converges to $(u_\infty, v_\infty, \psi_\infty)$ in V.
Since $t \longmapsto \mathcal{E}(u, \partial_t u, \psi)$ is continuous, we thus have

$$\begin{aligned}\lim_{t \to +\infty} \mathcal{E}(u, \partial_t u, \psi) &= \lim_{t \to +\infty} \mathcal{E}(Z(t)(u_0, u_1, 0)) \\ &= \lim_{t_k \to +\infty} \mathcal{E}(Z(t_k)(u_0, u_1, 0)) \\ &= \mathcal{E}(u_\infty, v_\infty, \psi_\infty).\end{aligned}$$

Moreover, for all positive s,

$$\begin{aligned}\lim_{t \to +\infty} \mathcal{E}(Z(t+s)(u_0, u_1, 0)) &= \lim_{t_k \to +\infty} \mathcal{E}(Z(s)Z(t_k)(u_0, u_1, 0)) \\ &= \mathcal{E}(Z(s)(u_\infty, v_\infty, \psi_\infty)).\end{aligned}$$

Then, if $(w, \partial_t w, \varphi) = Z(t)(u_\infty, v_\infty, \psi_\infty)$ denotes the solution to problem (11), with initial data $(u_\infty, v_\infty, \psi_\infty)$ in $D(A)$, we have $\mathcal{E}(w, \partial_t w, \varphi) = \mathcal{E}(u_\infty, v_\infty, \psi_\infty)$ for all positive t. Hence, according to the proof of Lemma 4.1, since

$$\frac{d}{dt}\mathcal{E}(w, \partial_t w, \varphi) = -\left[\int_\Sigma \frac{\kappa}{2}\left(\gamma - \frac{\kappa}{4}\right)|\varphi|^2\, d\sigma + \int_\Sigma |\partial_t w|^2\, d\sigma\right],$$

we necessarily have $\partial_t w = 0$ on Σ and $\varphi = 0$ on Σ. We then deduce that w is solution to the following problem

$$\begin{aligned}
&\partial_t^2 w - \Delta w = 0 && \text{in } \Omega \times [0, +\infty[\\
&w(x,0) = u_\infty,\ \partial_t w(x,0) = v_\infty && \text{in } \Omega \\
&w = 0 && \text{on } \Gamma \times [0, +\infty[\\
&\partial_n w = 0 && \text{on } \Sigma \times (0, +\infty)
\end{aligned}$$

and $z := \partial_t w$ is solution to

$$\begin{aligned}
&\partial_t^2 z - \Delta z = 0 && \text{in } \Omega \times [0, +\infty[\\
&z(x,0) = v_\infty,\ \partial_t z(x,0) = \Delta u_\infty && \text{in } \Omega \\
&z = 0 && \text{on } \Gamma \times [0, +\infty[\\
&\partial_n z = z = 0 && \text{on } \Sigma \times (0, +\infty)\,.
\end{aligned}$$

Since $\partial_n z = z = 0$ on Σ, we deduce that $z = 0$ in $\Omega \times [0, +\infty[$, as a consequence of the Holmgren theorem (see e.g. Lions [21]). Therefore, w is solution to

$$\begin{aligned}
&\Delta w = 0 && \text{in } \Omega \times [0, +\infty[\\
&w(x,0) = u_\infty && \text{in } \Omega \\
&w = 0 && \text{on } \Gamma \times [0, +\infty[\\
&\partial_n w = 0 && \text{on } \Sigma \times (0, +\infty)
\end{aligned}$$

which implies that $w = 0$ in $\Omega \times [0, +\infty[$ since Ω is connected. The pair (u_∞, v_∞) is thus equal to zero. Consequently, we also get that ψ_∞ is also equal to zero and *a fortiori*, we have $\mathcal{E}(u_\infty, v_\infty, \psi_\infty) = 0$. ◁

We are now willing to set

Theorem 4.4 *Let $(u_0, u_1, 0)$ in V. If (12) is satisfied, the solution u to (11) satisfies*

$$\lim_{t \to +\infty} (u, \partial_t u, \psi) = (0, 0, 0) \text{ in } H.$$

▷ Proof : If the pair $(u_0, u_1, 0)$ is in V, we know that $\lim_{t \to +\infty} \mathcal{E}(u, \partial_t u, \psi) = 0$ (cf. Theorem 4.3) and that $\mathcal{E}$ is a norm on H, equivalent to $\|\ \|$.
Therefore, $\lim_{t \to +\infty} (u, \partial_t u, \psi) = (0, 0, 0)$ in H. ◁

Theorem 4.4 is still valid when $\gamma = \frac{\kappa}{4}$. The result has been proved in [7].

5 Numerical Experiments

In this section, we analyze numerically the impact of the parameter γ on the accuracy of the ABC (Subsection 5.2), we compare the performance of the ABC to the performance of the BGT2 condition (Subsection 5.3), and we illustrate the exponential decay of the energy $\mathcal{E}$ (Subsection 5.4). To perform the experiments, we have discretized (11) by the Interior Penalty Discontinuous Galerkin (IPDG) method, which is described in the Subsection 5.1.

5.1 General setting of the IPDG method

The IPDG method, also known as Symmetric Interior Penalty (SIP) method, has been introduced in [6, 12] for general elliptic problems. It is a discontinuous Galerkin approximation method in which a penalization term is introduced to impose the weak continuity of the solution through each element of the mesh. As a Discontinuous Galerkin method, it allows to use block-diagonal (and thus easily invertible) matrices. Moreover, it has been shown in [5] that IPDG is one of the only Discontinuous Galerkin method that is both stable and consistant, which guarantees an optimal order of convergence.

We consider a triangulation $\mathcal{T}_h$ of Ω composed of elements K, triangles in 2D or tetrahedra in 3D. We denote by Ω_h the set of elements, by Σ_{abs} the set of the edges on the absorbing boundary Σ, by Σ_{D} the set of the edges on Γ and by Σ_{i} the set of the edges inside the domain. We thus have $\Sigma_{\text{i}} \cap (\Sigma_{\text{D}} \cup \Sigma_{\text{abs}}) = \varnothing$. For each $\sigma \in \Sigma_{\text{i}}$, two elements, denoted arbitrarily by K^+ and K^-, share σ. We define the jump and the average over each edge by:

$$[\![v]\!] := v^+\boldsymbol{\nu}^+ + v^-\boldsymbol{\nu}^- \qquad \text{and} \qquad \{\!\{v\}\!\} := \frac{v^+ + v^-}{2},$$

where v^+ and v^- respectively refer to the restriction of v in K^+ and K^- and $\boldsymbol{\nu}^{\pm}$ stands for the unit outward normal vector to $K^{\pm}$.

Regarding the external boundary condition, it reads as $\partial_n u = -\partial_t u - \frac{\kappa}{2}\psi$ on Σ, with $\left(\partial_t - \frac{\kappa}{4} + \gamma\right)\psi = \partial_t u$ on Σ.

We seek an approximation of the solution u in the finite element space V_h^k defined for $k \in \mathbb{N}$ by $V_h^k = \left\{v \in L^2(\Omega); v_{|K} \in P^k(K), \forall K \in \mathcal{T}_h\right\}, k \in \mathbb{N}$ and an approximation of ψ in the finite element space W_h^k defined by $W_h^k = \left\{w \in L^2(\Sigma); w_{|\sigma} \in P^k(\sigma), \forall \sigma \in \Sigma_{\text{ abs}}\right\}$ where $P^k(K)$ (respectively $P^k(\sigma)$) is the set of polynomials of degree at most k on K (respectively on σ).

The discrete problem is then given by

$$\begin{aligned}
&\text{Find } u_h \in V_h^k \times (0,+\infty) \text{ and } \psi \in W_h^k \times (0,+\infty) \text{ such that, } \forall (v_h, w_h) \in V_h^k \times W_h^k,\\
&\sum_{K\in\mathcal{T}_h}\int_K \partial_t^2 u_h v_h dx + a(u_h, v_h) + \sum_{\sigma\in\Sigma_{\text{abs}}}\int_\sigma \left(\partial_t u_h + \frac{\kappa}{2}\psi_h\right) v_h d\sigma = \sum_{K\in\mathcal{T}_h}\int_K S v_h dx,\\
&\sum_{\sigma\in\Sigma_{\text{abs}}}\int_\sigma \left(\partial_t - \frac{\kappa}{4} + \gamma\right)\psi_h w_h d\sigma = \sum_{\sigma\in\Sigma_{\text{abs}}}\int_\sigma \partial_t u_h w_h d\sigma,
\end{aligned}$$

with

$$a(u,v) = \sum_K \int_K \nabla u \nabla v dx - \sum_{\sigma\in\Sigma_{\text{i}}}\int_\sigma \Big(\{\!\{\nabla u\}\!\}\,[\![v]\!] + \{\!\{\nabla v\}\!\}\,[\![u]\!] - \frac{\alpha}{h_\sigma}[\![u]\!]\,[\![v]\!]\Big) d\sigma.$$

The function h_σ is the smallest radius of the inscribed circles of the two elements sharing σ and $\alpha \in \mathbb{R}^{+*}$ is a penalization coefficient [2]. We refer to [6, 5] for more details on IPDG methods, to [2, 1] for an analysis of the penalization coefficient and to [17] for the application of the IPDG method to the discretization of the wave equation.

We consider in the following two dimensional problems. Then, for each element K (resp. for each edge σ) the dimension of $P^k(K)$ (resp. $P^k(\sigma)$) is $n = C^k_{k+2}$ (resp. $m = k+1$). If the mesh is composed of N_e elements and N_f edges, we then have $N := N_e \times n$ degrees of freedom to interpolate u_h and $M := N_f \times m$ degrees of freedom to interpolate ψ_h.

If $\{v_i\,,\, 1 \leqslant i \leqslant N\}$ denotes a basis of V_h^k and $\{w_i\,,\, 1 \leqslant i \leqslant M\}$ is a basis of W_h^k, we set

$$u_h\,(x,t) = \sum_{i=1}^{N} U_i\,(t)\, v_i\,(x) \quad \text{and} \quad \psi_h\,(x,t) = \sum_{i=1}^{M} \Psi_i\,(t)\, w_i\,(x)\,.$$

The algebraic form of the problem is thus given by

$$\begin{aligned} &M\frac{d^2\mathbf{U}}{dt^2} + B\frac{d\mathbf{U}}{dt} + \frac{1}{2}B_\kappa\mathbf{\Psi} + K\mathbf{U} = \mathbf{S}, \\ &C\frac{d\mathbf{\Psi}}{dt} + C_{\kappa,\,\gamma}\mathbf{\Psi} = D\frac{d\mathbf{U}}{dt} \end{aligned} \tag{22}$$

where $\mathbf{U}$ and $\mathbf{\Psi}$ are the vectors of unknowns and

$$M = \left(\sum_{K\in\mathcal{T}_h}\int_K v_i v_j dx\right)_{1\leqslant i,j\leqslant N},\ K = (a(v_i,v_j))_{1\leqslant i,j\leqslant N}$$

$$B = \left(\sum_{\sigma\in\Sigma_{\rm abs}}\int_\sigma v_i v_j d\sigma\right)_{1\leqslant i,j\leqslant N},\ B_\kappa = \left(\sum_{\sigma\in\Sigma_{\rm abs}}\int_\sigma \kappa w_j v_i d\sigma\right)_{\substack{1\,\leqslant\, i\,\leqslant\, N\\ 1\,\leqslant\, j\,\leqslant\, M}}$$

$$C = \left(\sum_{\sigma\in\Sigma_{\rm abs}}\int_\sigma w_i w_j d\sigma\right)_{1\leqslant i,j\leqslant M},\ C_{\kappa,\,\gamma} = \left(\sum_{\sigma\in\Sigma_{\rm abs}}\int_\sigma \left(\gamma - \frac{\kappa}{4}\right) w_i w_j d\sigma\right)_{1\leqslant i,j\leqslant M},$$

$$D = \left(\sum_{\sigma\in\Sigma_{\rm abs}}\int_\sigma v_j w_i d\sigma\right)_{\substack{1\,\leqslant\, i\,\leqslant\, M\\ 1\,\leqslant\, j\,\leqslant\, N}},\ \mathbf{S} = \left(\sum_{K\in\mathcal{T}_h}\int_K S\, v_i dx\right)_{1\leqslant i\leqslant N}.$$

For the time discretization, we use a second-order finite difference scheme with a time step Δt and we obtain

$$\mathbf{M}\mathbf{X}^{n+1} = \begin{pmatrix} \Delta t^2\mathbf{S}^n \\ 0 \end{pmatrix} + \begin{pmatrix} -\Delta t^2 K + 2M \\ 0 \end{pmatrix}\mathbf{X}^n + \tilde{\mathbf{M}}\mathbf{X}^{n-1}, \tag{23}$$

where

$$\mathbf{M} = \begin{pmatrix} M + \dfrac{\Delta t}{2}B & \dfrac{\Delta t^2}{2}B_\kappa \\ -D & C + \Delta t C_{\kappa,\,\gamma} \end{pmatrix}, \tilde{\mathbf{M}} = \begin{pmatrix} -M + \dfrac{\Delta t}{2}B & -\dfrac{\Delta t^2}{2}B_\kappa \\ -D & C - \Delta t C_{\kappa,\,\gamma} \end{pmatrix}$$

$$\text{and } \mathbf{X}^i = \begin{pmatrix} \mathbf{U}^i \\ \mathbf{\Psi}^i \end{pmatrix}.$$

In the following numerical experiments, we use $\mathcal{P}^3$ elements and we choose $\alpha = 20$, $\Delta t = 0.05h$, where h denotes the radius of the circumscribed circle of the smallest cell of the mesh.

Remark 5.1 *In practice, we do not invert the matrix* $\mathbf{M}$ *and we solve (23) element by element. To simplify the presentation, we assume, without loss of generality, that the degrees of freedom are numbered such that*

1. *the element K_i is the support of functions $\left(v_{n(i-1)+j}\right)_{j=1,n}$;*

2. *the edge σ_i is the support of functions $\left(w_{m(i-1)+j}\right)_{j=1,m}$.*

We then denote by U_{K_i} (resp. Ψ_{σ_i}) the restrictions of U (resp. Ψ) to the element K_i (resp. the edge σ_i): $U_{K_i} = \left(U_{n(i-1)+j}\right)_{j=1,n}$, $\Psi_{\sigma_i} = \left(\Psi_{m(i-1)+j}\right)_{j=1,m}$, by M_{K_i} and B_{K_i} the restrictions of M and B to the element K_i :

$$M_{K_i} = \left(M_{n(i-1)+j,n(i-1)+k}\right)_{j,k=1,n}, \quad B_{K_i} = \left(B_{n(i-1)+j,n(i-1)+k}\right)_{j,k=1,n},$$

and by $B_{\kappa\sigma_i}$, C_{σ_i}, $C_{\kappa,\gamma_{\sigma_i}}$ and D_{σ_i} the restrictions of B_κ, C, $C_{\kappa,\gamma}$ and D to the edge σ_i.

$$B_{\kappa\sigma_i} = \left(B_{\kappa n(j_i-1)+k,m(i-1)+l}\right)_{\substack{k=1,n\\ l=1,m}}, \quad C_{\sigma_i} = \left(C_{m(i-1)+k,m(i-1)+l}\right)_{\substack{k=1,m\\ l=1,m}}$$
$$C_{\kappa,\gamma_{\sigma_i}} = \left(C_{\kappa,\gamma_{m(i-1)+k,m(i-1)+l}}\right)_{\substack{k=1,m\\ l=1,m}}, \quad D_{\sigma_i} = \left(D_{m(i-1)+k,n(j_i-1)+l}\right)_{\substack{k=1,m\\ l=1,n}}$$

(if we suppose that the edge i belongs to the element j_i).
Then,

1. *if K_i is an interior element (i.e. an element with no edge on Σ), we have to solve the system $M_{K_i} U_{K_i}^{n+1} = G$ where G is a vector that only depends on U^n, U^{n-1} and $\mathbf{S}^n$;*

2. *if K_i is a boundary element, with for instance two external edges σ_{j_1} and σ_{j_2} (in practice a boundary element has one or two external edge), we have to solve the system*

$$\begin{pmatrix} M_{K_i} + \frac{\Delta t}{2} B_{K_i} & \frac{\Delta t^2}{2} B_{\kappa\sigma_{j_1}} & \frac{\Delta t^2}{2} B_{\kappa\sigma_{j_2}} \\ -D_{\sigma_{j_1}} & C_{\sigma_{j_1}} + \Delta t C_{\kappa,\gamma_{\sigma_{j_1}}} & 0 \\ -D_{\sigma_{j_2}} & 0 & C_{\sigma_{j_2}} + \Delta t C_{\kappa,\gamma_{\sigma_{j_2}}} \end{pmatrix} \begin{pmatrix} U_{K_i}^{n+1} \\ \Psi_{\sigma_{j_1}}^{n+1} \\ \Psi_{\sigma_{j_2}}^{n+1} \end{pmatrix} = G$$

   where G is a vector that only depends on U^n, U^{n-1}, Ψ^n, Ψ^{n-1} and $\mathbf{S}^n$.

   If K_i has two external edges (resp. one), we thus have to invert a $(n+2m)\times(n+2m)$ matrix (resp. $(n+m)\times(n+m)$.

In all cases, we just have to solve small systems easily invertible.

Note that, in the particular case of the curvature condition (i.e $\gamma = \kappa/4$), we have $u = \psi$ and the system can be rewritten as

$$M\frac{d^2\mathbf{U}}{dt^2} + B\frac{d\mathbf{U}}{dt} + B_\kappa \mathbf{U} + \mathbf{K}\mathbf{U} = \mathbf{S}, \tag{24}$$

so that there is no need to compute the auxiliary variable.

5.2 Accuracy of the ABC

Now, we want to analyze the performances of the ABC (7) compared to the ones of the C-ABC which corresponds to $\gamma = \frac{\kappa}{4}$. To this aim, we will consider two configurations denoted respectively by Configuration 1 and Configuration 2. In Configuration 1, the two-dimensional domain Ω_1 (see Fig. 2) is delimited by a circular exterior boundary Σ_1 and the boundary Γ_1 represents the boundary of the obstacle. Both circles are centered at the origin. The radius of

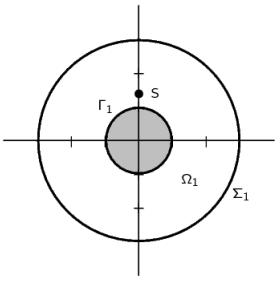

Figure 2: Computational domain - Configuration 1

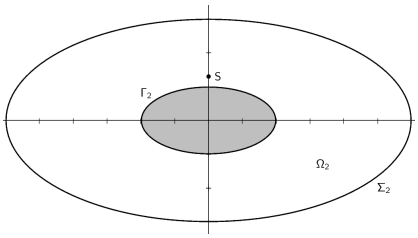

Figure 3: Computational domain - Configuration 2

Σ_1 is $R_{\text{ext}} = 3$m and the radius of Γ_1 is $R_{\text{int}} = 1$m. The point source S is set at (0m, 1.3m) and is defined as a second-derivative of a Gaussian with a dominant frequency f_0 of 1Hz:

$$S = \delta_{x_0} 2\lambda \left(\lambda \left(t - t_0\right)^2 - 1\right) e^{-\lambda (t-t_0)^2},$$

with $x_0 = (0\text{m}, 1.3\text{m})$, $\lambda = \pi^2 f_0^2$ and $t_0 = 1/f_0$. Since the source decays exponentially in time for $t \geqslant t_0$, we consider that $S(t) = 0$ for $t \geqslant 5t_0$

In Configuration 2, Ω_2 (see Fig. 3) is a two-dimensional domain delimited by an exterior boundary Σ_2 and by an interior boundary Γ_2. Σ_2 is an ellipse of semi-major axis $a_{\text{ext}} = 6$m and semi-minor axis $b_{\text{ext}} = 3$m centered in the origin. Γ_2 is the boundary of an elliptical obstacle of semi-major axis a =2m and semi-minor axis b =1m centered at the origin.

To compare the efficiency of the ABC (7) for different values of γ, we first compute the relative L^2-error in time at a given receiver set near the exterior boundary. To evaluate this relative error, we have to compute the exact solution at each receiver. We did not actually compute the exact solution, but we computed an approximate solution in a larger domain including Ω_1 and Ω_2. Indeed, we multiplied the dimensions of Σ_1 and Σ_2 by 3. The relative $L^2_{(x,y)}([0,T])$ error at point (x, y) is defined by

$$\frac{\left(\int_0^T (u_{app}(t,(x,y)) - u_{ex}(t,(x,y)))^2 dt\right)^{1/2}}{\left(\int_0^T (u_{ex}(t,(x,y)))^2 dt\right)^{1/2}}, \tag{25}$$

where u_{app} is the numerical solution and u_{ex} is the exact solution computed inside the large domain. The error is computed after 6000 time steps (with a time step equal to $3.6 * 10^{-3}$s).

We consider three receivers set near the boundary with coordinates (0, 2.85m), (0.7m, 2.75m) and (1.4m, 2.45m) for Configuration 1 and four receivers whose coordinates are (6m, 2.05m), (5m, 2.3m), (6m, −2.05m) and (5m, −2.3m) for Configuration 2. The results are given in Tab. 1 for Configuration 1 and Tab. 2 for Configuration 2. We can see that the relative L^2-error does not vary significantly with the values of γ and is similar to the errors obtained with the C-ABC ($\gamma = \frac{\kappa}{4}$). The error seems to increase when γ is greater than κ but does not grow fast.

For the next numerical tests, we fix $\gamma = \frac{\kappa}{4}$. Now, we interest ourselves on the evolution of the errors when moving the absorbing boundary. That is to find out where the boundary should be to obtain suitable results without high computational burdens. We first consider Configuration 1. We have tested six different radius R_{ext}: 1.5m, 2m, 3m, 4m, 5m and 6m in order to find the critical value of the radius of the exterior circle we should take to obtain accurate results.

	(0, 2.85m)	(0.7m, 2.75m)	(1.4m, 2.45m)
$\gamma = \frac{\kappa}{4}$	4.92	13.11	13.30
$\gamma = \frac{\kappa}{3}$	4.92	13.10	13.31
$\gamma = \kappa$	4.89	13.19	13.37
$\gamma = 3\kappa$	4.92	13.42	13.83
$\gamma = 10\kappa$	5.33	14.04	14.22

Table 1: Relative L^2 error (in %) - Source in (1.5,1) - Configuration 1

	(6m, 2.05m)	(5m, 2.3m)	(6m, −2.05m)	(5m, −2.3m)
$\gamma = \frac{\kappa}{4}$	2.49	3.65	6.77	11.53
$\gamma = \frac{\kappa}{3}$	2.49	3.65	6.79	11.56
$\gamma = \kappa$	2.50	3.66	6.93	11.75
$\gamma = 3\kappa$	2.52	3.67	7.35	12.31
$\gamma = 10\kappa$	2.60	3.74	7.89	13.10

Table 2: Relative L^2 error (in %) - Source in (1.5,1) - Configuration 2

First, we set three receivers of coordinates (1.025m, 1.025m), (1.256m, 0.725m) and (1.4m, 0.375m) near the obstacle and we evaluate the relative L^2-error in time defined in (25). The results we have obtained are presented in Tab. 3. We see that, when the artificial boundary is set

	(1.025m, 1.025m)	(1.256m, 0.725m)	(1.4m, 0.375m)
$R_{\text{ext}} = 1.5$m	29.87	35.08	41.75
$R_{\text{ext}} = 2$m	6.49	10.84	18.17
$R_{\text{ext}} = 3$m	1.46	2.46	4.52
$R_{\text{ext}} = 4$m	0.96	1.42	2.03
$R_{\text{ext}} = 5$m	0.94	1.33	1.11
$R_{\text{ext}} = 6$m	0.93	0.87	1.07

Table 3: Relative L^2 error (in %) - Source in (1.3,0) - Configuration 1

near the boundary of the obstacle, the relative errors are very important because the amplitude of reflected waves is high. When the radius of the artificial boundary is greater than 3m, we obviously obtain small relative errors because the reflected waves are generated by propagating waves impinging the external boundary with a low amplitude. We can observe that the error level stabilizes around 1% as soon as $R_{\text{ext}} \geqslant 3m$. Therefore, when the obstacle is a circle we recommend to take for the artificial boundary a circle whose radius is equal to three times the radius of the obstacle. Let us precise that the same conclusion holds for any value of γ greater than $\frac{\kappa}{4}$.

Now, we perform the same kind of analysis but looking at the global error in space and in

time, i.e. we evaluate the global relative $L^2([0,t]\times\Omega)$-error defined by

$$\left(\frac{\displaystyle\int_0^t\int_\Omega |u_{app}(s,x)-u_{ex}(s,x)|^2 dxds}{\displaystyle\int_0^t\int_\Omega |u_{ex}(s,x)|^2 dxds}\right)^{1/2}.$$

By this way, the impact of measures near the external boundary is averaged and we thus get a better illustration of the accuracy of the solution. In order to compare accurately this error, we used the same time step for computing both the approximate and the reference solution. The results we have obtained are presented in Fig. 4. For external radius smaller than 3m, the computed relative errors are between 5 and 25%. When the external radius is greater than 4m, we obtain small relative errors around 2.5% and 1%. Hence, choosing an external radius of 4m when the interior radius is equal to 1m seems to be again the best choice to obtain good approximations of the solution of the wave equation without high computation burdens. Now,

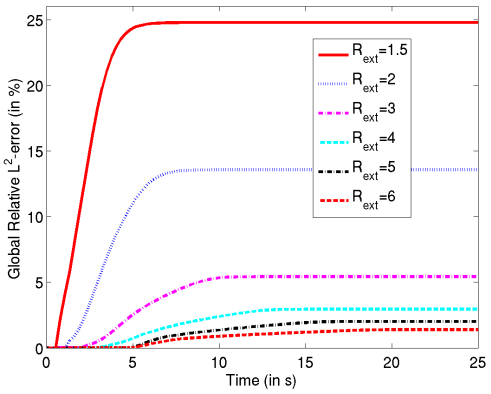

Figure 4: Global relative error for different distances to the obstacle - Configuration 1

let us consider the case of an elliptic obstacle. Here again, we consider six different domains in which the external boundary is set further and further away from the obstacle. In each case, the interior boundary is the same as in Configuration 2. The exterior boundary is then an ellipse centered in the origin of semi-major axis a_{ext} and semi-minor axis b_{ext}. a_{ext} and b_{ext} are respectively obtained by multiplying a and b by 1.5, 2, 3, 4, 5 and 6. We have set three receivers near the obstacle of coordinates (0.75m, 1.4m), (2.51m, 0.725m) and (2.8m, 0.375m) and we evaluate the relative L^2-error in time defined in (25). The results we have obtained are displayed in Tab. 4. In this case, we obtain really good results when $a_{\text{ext}} \geqslant 4a$ and $b_{\text{ext}} \geqslant 4b$. If we take $a_{\text{ext}} = 6$m and $b_{\text{ext}} = 3$m we obtain suitable results but the difference with the case when $a_{\text{ext}} = 8$m and $b_{\text{ext}} = 4$m is important. Next, we compute the relative $L^2([0,t]\times\Omega)$-error. The results are depicted in Fig. 5. We deduce that in such a configuration, we should take $a_{\text{ext}} = 3a$ and $b_{\text{ext}} = 3b$ to obtain small relative errors as in the case of a circular scatterer. In these numerical experiments, we have not observed any instabilities even in long-term simulations.

	(0.75m, 1.4m)	(2.51m, 0.725m)	(2.8m, 0.375m)
$a_{\text{ext}} = 3\text{m}$, $b_{\text{ext}} = 1.5\text{m}$	35.03	61.61	69.34
$a_{\text{ext}} = 4\text{m}$, $b_{\text{ext}} = 2\text{m}$	4.27	22.69	30.77
$a_{\text{ext}} = 6\text{m}$, $b_{\text{ext}} = 3\text{m}$	4.1	8.75	10.52
$a_{\text{ext}} = 8\text{m}$, $b_{\text{ext}} = 4\text{m}$	3.72	2.48	3.27
$a_{\text{ext}} = 10\text{m}$, $b_{\text{ext}} = 5\text{m}$	0.59	1.15	1.77
$a_{\text{ext}} = 12\text{m}$, $b_{\text{ext}} = 6\text{m}$	0.44	0.55	1.38

Table 4: Relative L^2 error (in %) - Source in (1.3,0) - Configuration 2

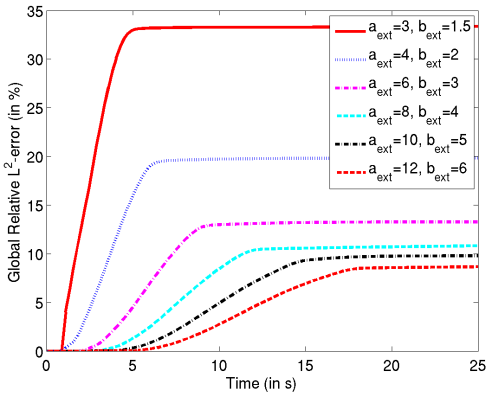

Figure 5: Global relative error for different distances to the obstacle - Configuration 2

5.3 Comparison with BGT2 condition

In this Subsection, we compare the performance of the curvature ABC with the performance of a BGT2 condition for arbitrarily convex surfaces. This condition reads as

$$\partial_n u + \partial_t u + \frac{\kappa(s)}{2}u - \frac{\kappa(s)}{8}\left(1+\frac{\partial_t}{\kappa(s)}\right)^{-1} u + \frac{\partial_s^2\kappa(s)}{8}(\partial_t^2)^{-1} - \partial_s\left(\frac{\left(1+\frac{\partial_t}{\kappa(s)}\right)^{-1}}{2\kappa(s)}\partial_s\right)u = 0, \quad (26)$$

where s denotes the curvilinear abscissa of the artificial boundary. We call it BGT2 condition since it is obtained from a classical BGT2 condition [4] for the Helmholtz equation :

$$\partial_n u - iku + \frac{\kappa(s)}{2}u - \frac{\kappa(s)}{8\left(1-\frac{ik}{\kappa(s)}\right)}u - \frac{\partial_s^2\kappa(s)}{8k^2} - \partial_s\left(\frac{1}{2\kappa(s)\left(1-\frac{ik}{\kappa(s)}\right)}\partial_s\right)u = 0, \quad (27)$$

where k denotes the frequency of the monochromatic wave.

The time-domain formulation of this condition involves the inversions of time derivative operators. To avoid these inversions, we reformulate (26) by introducing two auxiliary unknowns defined only on the artificial boundary Σ :

$$\begin{cases} \partial_n u + \partial_t u + \dfrac{\kappa}{2}u - \psi_1 - \psi_2 = 0, \\ \kappa\psi_1 + \partial_t\psi_1 - \dfrac{\kappa^2}{8}u - \dfrac{1}{2}\partial_s^2 u = 0, \\ \partial_t^2\psi_2 + \dfrac{\partial_s^2\kappa}{8}u = 0. \end{cases} \quad (28)$$

We explain in the appendix how we derived this condition and how we implemented it in the IPDG formulation. Because of the second order derivative with respect to the curvature, the implementation of this condition requires the introduction of an additional penalty parameter on the absorbing boundary.

Note that, in the particular case where the boundary is a circle of radius R, the term $\partial_s^2\kappa$ vanishes and we only need to compute the auxiliary variable ψ_1.

In Fig. 6, we represent the global relative error obtained for the first configuration (the circle) for $R_{ext} = 1.5, 2, 3, 4, 5$ and 6.

We remark that, compared to Fig. 4, the BGT2 condition improves the accuracy of the solution for $R_{ext} = 1.5$ and 2. However, the errors are still greater than 10%. For $R_{ext} \geqslant 3$, there is no significant improvement. This means that, in order to obtain an accuracy around 1%, it is still necessary to choose $R_e xt \geqslant 4$, and the curvature condition should be preferred since it does not involve an auxiliary variable.

In Fig. 7, we represent the global relative error obtained for the second configuration (the ellipse) for $(a_{ext}, b_{ext}) = (3, 1.5), (4, 2), (6, 3), (8, 4), (10, 5)$ and $(12, 6)$. In this configuration, the BGT2 condition improves the accuracy of the solution whatever the distance between the boundary and the obstacle is, even if this improvement is less important when the distance increases. However, the solution is long-term unstable in the case $(a_{ext}, b_{ext}) = (3, 1.5)$. To emphasize this fact, we have represented this solution on a larger time interval in Fig. 8. We have also represented the solution obtained with $(a_{ext}, b_{ext}) = (4, 2)$ in Fig. 9

It does not necessarily mean that the continuous problem corresponding to the BGT2 condition is unstable. It may also mean that the numerical scheme that we employ may be not

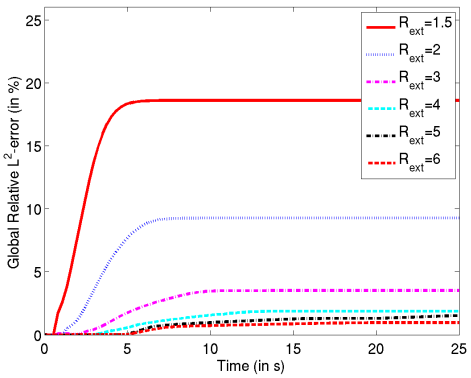

Figure 6: Global relative error for different distances to the obstacle, using BGT2 condition - Configuration 1

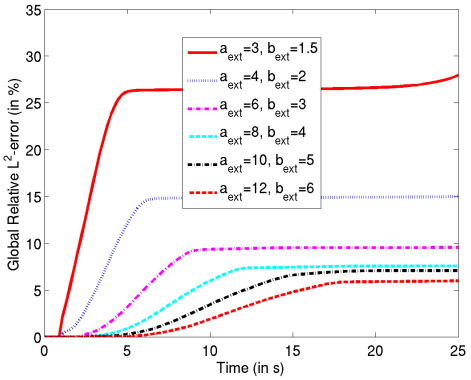

Figure 7: Global relative error for different distances to the obstacle, using BGT2 condition - Configuration 2

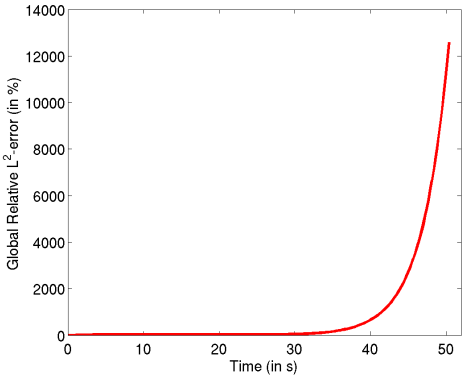

Figure 8: Global relative error for $(a_{ext}, b_{ext}) = (3, 1.5)$ using BGT2 condition on a larger time interval - Configuration 2

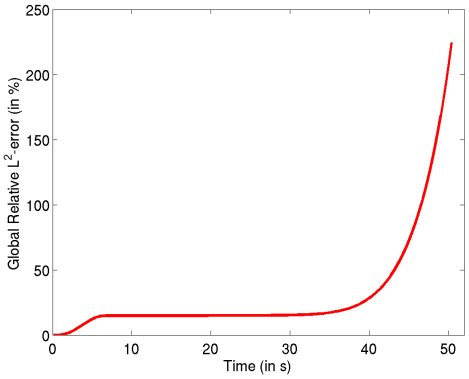

Figure 9: Global relative error for $(a_{ext}, b_{ext}) = (4, 2)$ using BGT2 condition on a larger time interval - Configuration 2

able to compute the solution with BGT2 condition. One solution could be to use an implicit time-scheme instead of the Leap-Frog scheme in the whole domain. This would require the inversion of a huge matrix at each time step, which, added to the fact that we have to compute two auxiliary variables on the interface, would increase too strongly the computational costs.

As a conclusion, we recommend to use the curvature condition instead of the BGT2 condition, since this latter increases the computational costs and is unstable when coupled with an IPDG scheme. However, the experiments we have presented have been performed on relatively short time, and they do not prove the long-term stability of the curvature condition. This is the object of the next Subsection.

5.4 Behavior of the discrete energy

In this Subsection, we illustrate the time behavior of the energy $\mathcal{E}$ defined at (19). To this aim, we first introduce the discrete energy corresponding to $\mathcal{E}$.

For $n \in \mathbb{N}$, we set

$$\begin{aligned} E^{n+1/2} &= \left(M \frac{\mathbf{U}^{n+1} - \mathbf{U}^n}{\Delta t}, \frac{\mathbf{U}^{n+1} - \mathbf{U}^n}{\Delta t} \right) + \left(K\mathbf{U}^{n+1}, \mathbf{U}^n \right) \\ &\quad + \frac{1}{2} \left[\left(C_\kappa \mathbf{\Psi}^{n+1}, \mathbf{\Psi}^{n+1} \right) + \left(C_\kappa \mathbf{\Psi}^n, \mathbf{\Psi}^n \right) \right] \end{aligned} \tag{29}$$

with $C_\kappa = \left(\sum_{\sigma \in \Sigma_{\text{abs}}} \int_\sigma \frac{\kappa}{2} v_i v_j \right)_{1 \leqslant i,j \leqslant M}$.

We consider the Configuration 1. We first want to illustrate that the discrete energy is decreasing when the source is switched off. In a second part, we illustrate the fact that the condition $\gamma \geqslant \frac{\kappa}{4}$ is an optimal condition to ensure the stability of the problem. In the last part, we show that the decay rate of the discrete energy seems to be exponential.

5.4.1 Energy decay

In Fig. 10, we represent the evolution of the discrete energy along the time when $\gamma = \kappa$. We see that the energy first increases, as long as the source is injecting some energy inside the system. Once $S(t) = 0$ (i.e. for $t \geqslant 5t_0$), the energy is constant as long as the wave has not reached the boundary of the domain. Finally, the energy starts decreasing as predicted by Theorem 4.3.

5.4.2 Stability of the ABC

Theorem 4.3 states that the problem is long-term stable if γ is greater than $\frac{\kappa}{4}$. We have performed some numerical experiments when the condition $\gamma \geqslant \frac{\kappa}{4}$. For example, if we take $\gamma = 0.1\kappa$, the system is unstable as we can see in Fig. 11. To illustrate the property that $\frac{\kappa}{4}$ is a critical value for γ, we compare the evolution of the discrete energy for $\gamma = 0.249\kappa$ and $\gamma = 0.25\kappa$. In Fig. 12 (resp. in Fig. 13), we depict the evolution of the discrete energy during 1 000 000 iterations when $\gamma = 0.249\kappa$ (resp. when $\gamma = 0.25\kappa$). If we give these figures a cursory glance, both systems seems to be stable for long-term, even when $\gamma < \frac{\kappa}{4}$. But if we look at Fig. 14 (resp. Fig. 15) where we have magnified the y-scale by a factor 10^4, for $\gamma = 0.249\kappa$ (resp. when $\gamma = 0.25\kappa$), we see that the scheme is not stable when $\gamma < \frac{\kappa}{4}$. The numerical tests thus indicate that $\frac{\kappa}{4}$ could be critical value for γ.

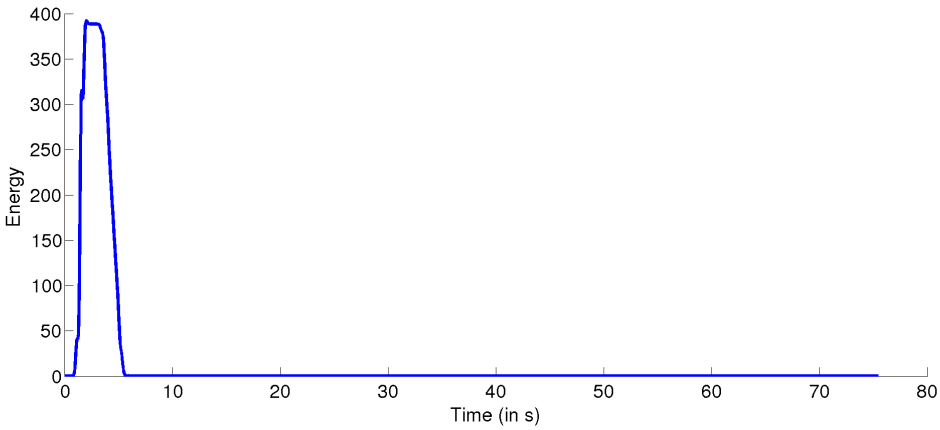

Figure 10: Energy vs time for $\gamma = \kappa$

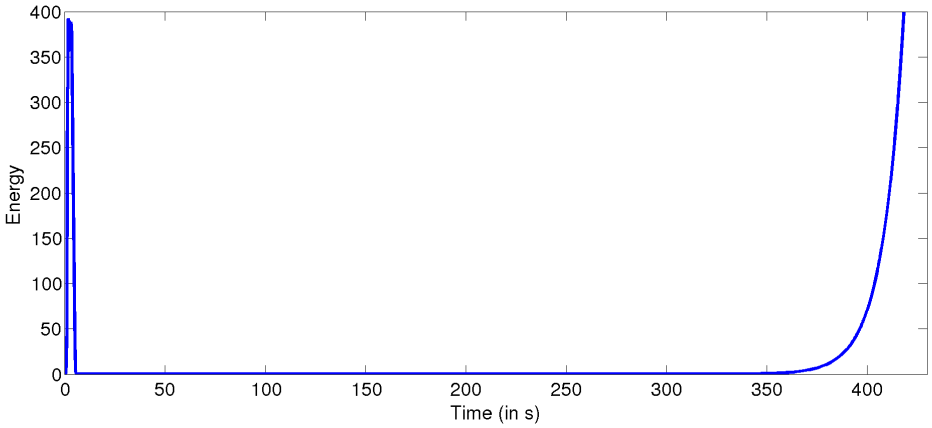

Figure 11: Energy vs time for $\gamma = 0.1\kappa$

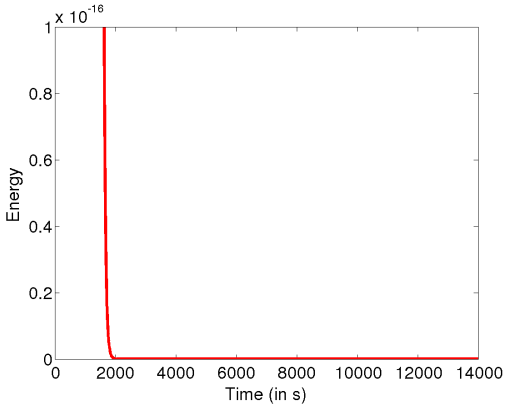

Figure 12: Energy for $\gamma = 0.249\kappa$

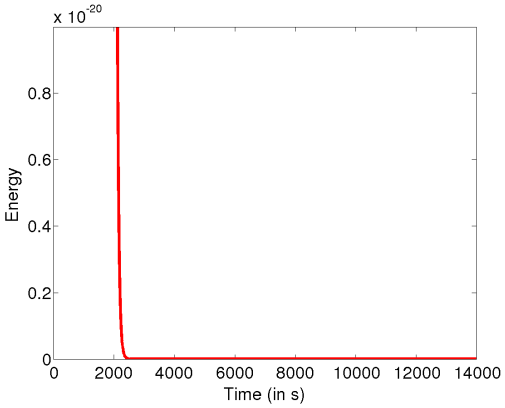

Figure 13: Energy for $\gamma = 0.25\kappa$

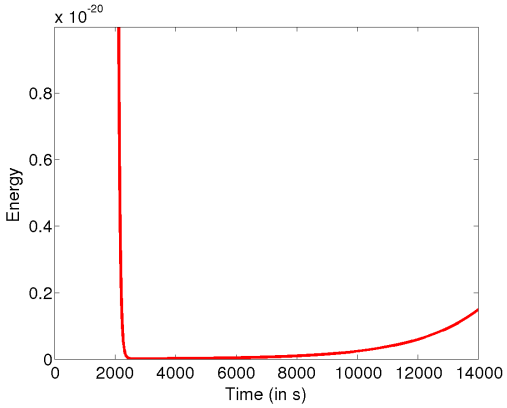

Figure 14: Energy for $\gamma = 0.249\kappa$ - y-scale magnified by 10^4

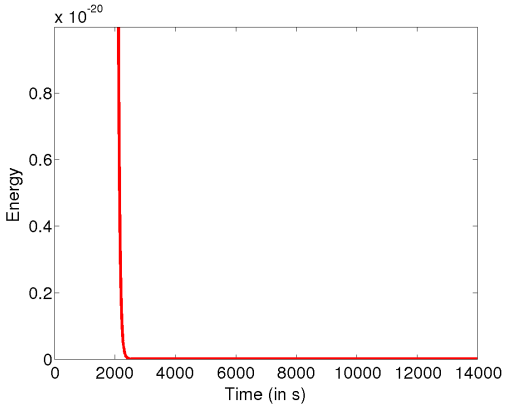

Figure 15: Energy for $\gamma = 0.25\kappa$ - y-scale magnified by 10^4

5.4.3 Exponential decay of the discrete energy

Theorem 4.3 ensures that the energy $\mathcal{E}$ is decreasing. In practice, its discrete equivalent is actually exponentially decreasing. To illustrate this property, we have computed the evolution of the logarithm of the discrete energy (see Fig. 16). Let us remark that the logarithm of the energy decreases linearly until $t = 250s$ and is constant for $t > 250s$. This is due to the fact that the energy becomes smaller than 10^{-16} and thus smaller than the round-off error. Using a linear regression method, we found that the logarithm of the energy could be approximated, for $t < 250s$ by the function $h(t) = -3 - 0.14t$, so that the energy could be approximated by the function $g(t) = exp(-0.14 * t - 3))$. These coefficients depends probably on the curvature

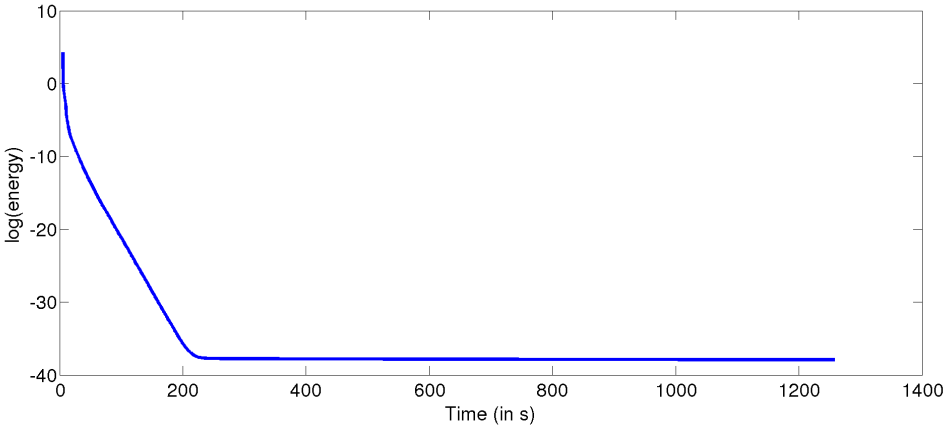

Figure 16: Log(energy) vs time for $\gamma = \kappa$

of the artificial boundary and of its distance to the obstacle. A more detailed numerical study will be necessary to analyze this dependence, but it is outside the scope of this paper. In Fig. 17, we compare the evolution of the discrete energy obtained with $\gamma = \kappa$ (black curve) with the function g (blue dashed curve), the y scale is magnified by 100 in the second picture and by 10^8 in the third one. It is clear that g is always greater than the discrete energy which seems to

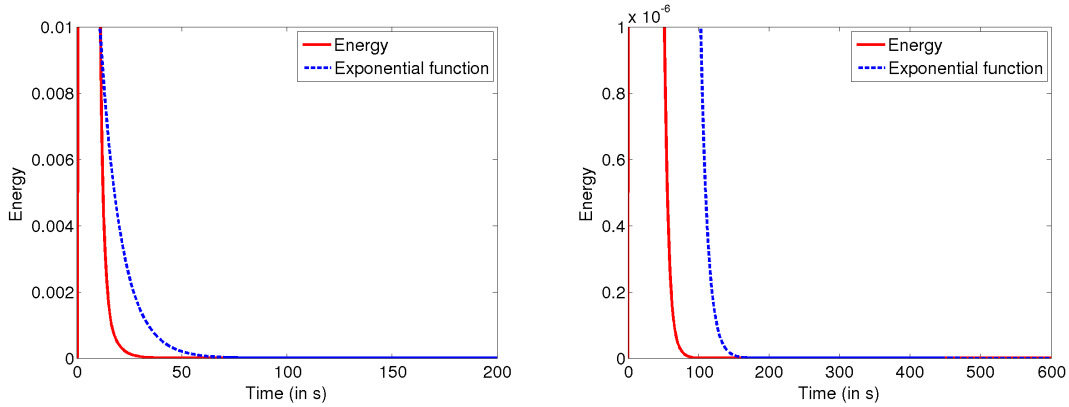

indicate that the energy could be exponentially decreasing.

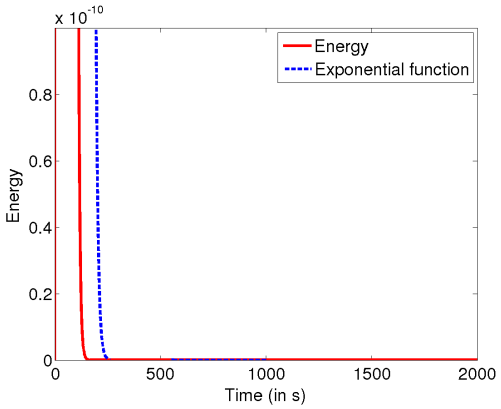

Figure 17: Exponential decay of the energy

6 Conclusion

We have constructed a new family of ABCs depending on a parameter γ. When $\gamma \geqslant \frac{\kappa}{4}$, the ABCs satisfy each criterion defined in the introduction. In particular, we have proved that there exists a functional of time which is an energy when $\gamma \geqslant \frac{\kappa}{4}$ and which is decreasing to zero. The numerical experiments that we have performed did not allow us to define that there exists a best ABC among the family of conditions. Nevertheless, our study let conclude that the C-ABC, which involves one-order differential operators, performs as well as the family of ABCs with $\gamma > \frac{\kappa}{4}$. Moreover, the C-ABC performs as well as the BGT2 condition and is long-term stable when coupled with IPDG method and Leap-Frog scheme, contrary to BGT2 condition. It would be now interesting to prove that the energy is actually exponentially decreasing. This result is already known for the C-ABC [7, 21] and it might be satisfied for the full family of ABC with $\gamma \geqslant \frac{\kappa}{4}$.

A Implementation of the BGT2 condition in the IPDG formulation

We describe here how we obtain condition (28) with auxiliary variables from condition 26 and how we implement it in the IPDG formulation. The main issue is the term $\partial_s \left(\frac{\left(1+\frac{\partial_t}{\kappa(s)}\right)^{-1}}{2\kappa(s)} \partial_s \right) u$. In the harmonic case, when ∂_t is replaced by $-ik$, this term can be easily taken into account into a variational formulation. This is unfortunately not possible for the transient wave equation, since the inverse of the operator $1 + \frac{\partial_t}{\kappa(s)}$ has to be computed via an auxiliary unknown.

One solution could be to rewrite the above term as

$$\partial_s \left(\frac{\left(1 - \frac{ik}{\kappa(s)}\right)^{-1}}{2\kappa(s)} \right) u + \frac{\left(1 - \frac{ik}{\kappa(s)}\right)^{-1}}{2\kappa(s)} \partial_s^2 u.$$

However, the first term would break the symmetry of the IPDG formulation and we prefer to approximate the curvature by a function which is constant on each edge. To do so, for each

edge σ on the boundary, we denote by s_σ^1 and s_σ^2 the curvilinear coordinates of the two nodes of σ and we define $\kappa_\sigma = (\kappa(s_\sigma^1) + \kappa(s_\sigma^2))/2$. This simplification will also be useful for the numerical computation of the integrals on the boundary. In the same way, we define $\partial_s^2\kappa_\sigma = (\partial_s^2\kappa(s_\sigma^1) + \partial_s^2\kappa(s_\sigma^2))/2$ and the approximated BGT2 condition on an external edge σ reads as

$$\partial_n u + \partial_t u + \frac{\kappa_\sigma}{2}u - \frac{\kappa_\sigma}{8}\left(1+\frac{\partial_t}{\kappa_\sigma}\right)^{-1} u + \frac{\partial_s^2\kappa_\sigma}{8}(\partial_t^2)^{-1}u - \frac{\left(1+\frac{\partial_t}{\kappa_\sigma}\right)^{-1}}{2\kappa_\sigma}\partial_s^2 u = 0. \tag{30}$$

Now, following the methodology we used above, we introduce two auxiliary variables ψ_1 and ψ_2 and we rewrite the condition as

$$\begin{cases} \partial_n u + \partial_t u + \dfrac{\kappa_\sigma}{2}u - \psi_1 - \psi_2 = 0, \\ \kappa_\sigma\psi_1 + \partial_t\psi_1 - \dfrac{\kappa_\sigma^2}{8}u - \dfrac{1}{2}\partial_s^2 u = 0 \\ \partial_t^2\psi_2 + \dfrac{\partial_s^2\kappa_\sigma u}{8} = 0. \end{cases} \tag{31}$$

Note that when the boundary is a circle, there is no need to introduce the second auxiliary variable ψ_2. To discretize the operator $\partial_s^2 u$ by the IPDG method, we introduce the bilinear form

$$a_2(u,v) = \sum_{\sigma\in\Sigma_{\rm i}}\left(\int_\sigma \partial_s u\partial_s v ds - \{\!\{\nabla u\}\!\}_{s_\sigma^1}[\![v]\!]_{s_\sigma^1} + \{\!\{\nabla v\}\!\}_{s_\sigma^1}[\![u]\!]_{s_\sigma^1} - \frac{\alpha_2}{h_\sigma}[\![u]\!]_{s_\sigma^1}[\![v]\!]_{s_\sigma^1}\right),$$

where $[\![u]\!]_{s_\sigma^1}$ and $\{\!\{u\}\!\}_{s_\sigma^1}$ denote respectively the jump and the mean value of u at point $\mathbf{x}(s_\sigma^1)$.

We obtain the algebraic system

$$\begin{aligned} &M\frac{d^2\mathbf{U}}{dt^2} + B\frac{d\mathbf{U}}{dt} - D^T(\mathbf{\Psi}_1 + \mathbf{\Psi}_2) + K\mathbf{U} = \mathbf{S}, \\ &C_\kappa\frac{d\mathbf{\Psi}_1}{dt} + C\mathbf{\Psi}_1 + K_\kappa\mathbf{U} = 0, \\ &C\frac{d^2\mathbf{\Psi_2}}{dt^2} + \mathbf{U} = 0, \end{aligned} \tag{32}$$

where

$$C_\kappa = \left(\sum_{\sigma\in\Sigma_{\rm abs}}\int_\sigma \kappa_\sigma w_i w_j d\sigma\right)_{1\leqslant i,j\leqslant M}, \quad K_\kappa = (a_2(v_i,v_j))_{1\leqslant i,j\leqslant M},$$

$$B_{\partial^2\kappa} = \left(\sum_{\sigma\in\Sigma_{\rm abs}}\int_\sigma \partial_s^2\kappa w_j v_i d\sigma\right)_{\substack{1\leqslant i\leqslant M\\ 1\leqslant j\leqslant N}}.$$

and the other matrices have been defined above.

We first chose to use a classical Leap-Frog scheme in the whole domain and the fully discretized

system reads as

$$\begin{aligned}
&M\frac{\mathbf{U}^{n+1}-2\mathbf{U}^{n}+\mathbf{U}^{n-1}}{\Delta t^2}+B\frac{\mathbf{U}^{n+1}-\mathbf{U}^{n-1}}{\Delta t}\\
&-D^T\left(\frac{{\boldsymbol{\Psi}_1}^{n+1}+{\boldsymbol{\Psi}_1}^{n-1}}{2}+\frac{{\boldsymbol{\Psi}_2}^{n+2}+{\boldsymbol{\Psi}_2}^{n-1}}{2}\right)+K\mathbf{U}^{n}=\mathbf{S}^{n},\\
&C_\kappa\frac{{\boldsymbol{\Psi}_1}^{n+1}-{\boldsymbol{\Psi}_1}^{n-1}}{\Delta t}+C\frac{{\boldsymbol{\Psi}_1}^{n+1}+{\boldsymbol{\Psi}_1}^{n-1}}{2}+K_\kappa\mathbf{U}^{n}=0,\\
&C\frac{\boldsymbol{\Psi}_2^{n+1}-2\boldsymbol{\Psi}_2^{n}+\boldsymbol{\Psi}_2^{n-1}}{\Delta t^2}+\frac{\mathbf{U}^{n+1}+\mathbf{U}^{n-1}}{2}=0.
\end{aligned}\tag{33}$$

Note that this system is implicit on the interface. However, since matrices M, B, D, C_κ are block-diagonal, we do not have to invert a global linear system but a linear system on each element of the boundary.

However, the second penalty parameter hampers the CFL condition of the global system and we observed instabilities, even in the case of a circular boundary. To circumvent this problem, we decided to approximate the term $K_\kappa\mathbf{U}$ by its mean value and we obtained the system

$$\begin{aligned}
&M\frac{\mathbf{U}^{n+1}-2\mathbf{U}^{n}+\mathbf{U}^{n-1}}{\Delta t^2}+B\frac{\mathbf{U}^{n+1}-\mathbf{U}^{n-1}}{\Delta t}\\
&-D^T\left(\frac{{\boldsymbol{\Psi}_1}^{n+1}+{\boldsymbol{\Psi}_1}^{n-1}}{2}+\frac{{\boldsymbol{\Psi}_2}^{n+2}+{\boldsymbol{\Psi}_2}^{n-1}}{2}\right)+K\mathbf{U}^{n}=\mathbf{S}^{n},\\
&C_\kappa\frac{{\boldsymbol{\Psi}_1}^{n+1}-{\boldsymbol{\Psi}_1}^{n-1}}{\Delta t}+C\frac{{\boldsymbol{\Psi}_1}^{n+1}+{\boldsymbol{\Psi}_1}^{n-1}}{2}+K_\kappa\frac{\mathbf{U}^{n+1}+\mathbf{U}^{n-1}}{2}=0,\\
&C\frac{\boldsymbol{\Psi}_2^{n+1}-2\boldsymbol{\Psi}_2^{n}+\boldsymbol{\Psi}_2^{n-1}}{\Delta t^2}+\frac{\mathbf{U}^{n+1}+\mathbf{U}^{n-1}}{2}=0.
\end{aligned}\tag{34}$$

Since the matrix K_κ is not block-diagonal, we can not solve this system element by element. However, the linear system involves only the unknowns on the absorbing boundary.

References

[1] C. Agut and J. Diaz. Stability analysis of the interior penalty discontinuous galerkin method for the wave equation. Technical Report 7494, INRIA Research Report, 2010.

[2] M. Ainsworth, P. Monk, and W. Muniz. Dispersive and dissipative properties of discontinuous galerkin finite element methods for the second-order wave equation. *J. Sci. Comp.*, 1-3:5–40, 2006.

[3] X. Antoine and H. Barucq. Microlocal diagonalization of strictly hyperbolic pseudodifferential systems and application to the design of radiation conditions in electromagnetism. *SIAM J. Appl. Math*, 61:1877–1905, 2001.

[4] X. Antoine, H. Barucq, and A. Bendali. Bayliss-turkel like radiation conditions on surfaces of arbitrary shape. *J. Math. Anal. Appl.*, 229, 1999.

[5] D. N. Arnold, F. Brezzi, B. Cockburn, and L. D. Marini. Unified analysis of disconitnuous galerkin methods for elliptic problems. *SIAM J. Numer. Anal.*, 39:1749–1779, 2002.

[6] D.N. Arnold. An interior penalty finite element method with discontinuous elements. *SIAM J. Num. Anal.*, 19(4):742–760, 1982.

[7] C. Bardos, G. Lebeau, and J. Rauch. Sharp sufficient conditions for the observation, control, and stabilization of waves from the boundary. *SIAM J. Control Optim.*, 30(5):1024–1065, 1992.

[8] H. Barucq. A new family of first-order boundary conditions for the maxwell system : derivation, well-posedness and long-time behavior,. *J. Math. Pure. Appl.*, 82:67–88, 2002.

[9] H. Barucq, J. Diaz, and V. Duprat. A new family of second-order absorbing boundary conditions for the acoustic wave equation - Part I: Construction and mathematical analysis, `http://hal.inria.fr/inria-00570301`. Technical Report 7553, INRIA Research Report, 2011.

[10] H. Barucq, J. Diaz, and V. Duprat. Micro-differential boundary conditions modelling the absorption of acoustic waves by 2d arbitrarily-shaped convex surfaces. *Communications in Computational Physics*, 11(2):674–690, 2012.

[11] H. Barucq and B. Hanouzet. Etude asymptotique du système de maxwell en dimension deux d'espace avec la condition aux limites absorbante de silver-müller. *C. R. Acad. Sci., Série I*, 316:547–552, 1993.

[12] F. Bassi and S. Rebay. A high-order accurate discontinuous finite element method for the numerical solution of the compressible navier-stokes equations. *J. Comput. Phys.*, 131:267–279, 1997.

[13] A Bayliss, M Gunzburger, and E Turkel. Boundary conditions for the numerical solution of elliptic equations in exterior regions. *SIAM Journal on Applied Mathematics*, 42(2):430–451, 1982.

[14] B. Engquist and A. Majda. Absorbing boundary conditions for the numerical simulation of waves. *Math. Comp.*, 31:629–651, 1977.

[15] D. Givoli and B. Neta. High-order non-reflecting boundary scheme for time-dependent waves. *Journal of Computational Physics*, 186(1):24 – 46, 2003.

[16] M.J. Grote and J.B. Keller. Exact nonreflecting boundary conditions for the time dependent wave equation. *SIAM J. Appl. Math.*, 55(2):280–297, 1995.

[17] M.J. Grote, A. Schneebeli, and D. Schötzau. Discontinuous galerkin finite element method for the wave equation. *SIAM J. Num. Anal.*, 44:2408–2431, 2006.

[18] R. Higdon. Numerical absorbing boundary conditions for the wave equation. *Math. Comp.*, 49:65–90, 1987.

[19] L. Hörmander. Pseudodifferential operators and hypoelliptic equations. *AMS Proc. Sym. Pure Math*, pages 138–183, 1967.

[20] T. Kato. *Perturbation Theory for Linear Operators*, volume 132. Springer-Verlag, 1966.

[21] J. L. Lions. *Contrôlabilité exacte, perturbations et stabilisation de systèmes distribués, T.1: Contrôlabilité exacte*. Masson, 1988.

[22] L. Nirenberg. Pseudodifferential operators and some applications. In *CMBS Regional Conf. Ser. in Math.*, volume 17 of *Lectures on Linear Partial Differential Equations*, pages 19–58. AMS, 1973.

[23] M. Sesquès. *Conditions aux limites artificielles pour le système de Maxwell.* PhD thesis, Université Bordeaux I, 1990.

[24] M.E. Taylor. *Pseudodifferential Operators.* Princeton University Press, 1981.

[25] Complete Radiation Boundary Conditions: Minimizing the Long Time Error Growth of Local Methods. T. hagstrom and t. warburton. *SIAM J. Numer. Anal.*, 47(5):3678–3704, 2009.

[26] L. N. Trefethen and L. Halpern. Well-posedness of one-way wave equations and absorbing boundary conditions. *Mathematics of Computation*, 47(176):421–435, 1986.

[27] S.V. Tsynkov. Numerical solution of problems on unbounded domains. a review. *Appli. Num. Math.*, pages 465–532, 1998.

Contents

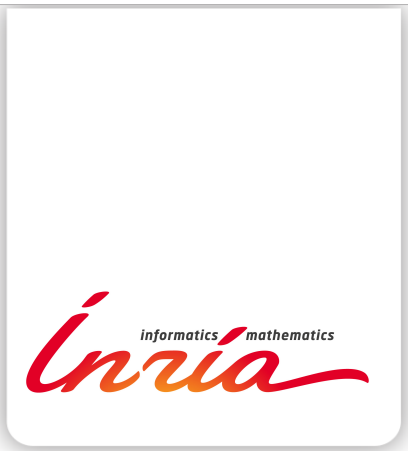

RESEARCH CENTRE
BORDEAUX – SUD-OUEST

200, Avenue de la Vieille Tour
33405 Talence Cedex

Publisher
Inria
Domaine de Voluceau - Rocquencourt
BP 105 - 78153 Le Chesnay Cedex
inria.fr

ISSN 0249-6399